



Universiteit  
Leiden  
The Netherlands

## Studying measures for interpersonal synchrony in brain response by means of applying graph theory measures to EEG data

Foegel, M.T.J.

### Citation

Foegel, M. T. J. (2022). *Studying measures for interpersonal synchrony in brain response by means of applying graph theory measures to EEG data.*

Version: Not Applicable (or Unknown)

License: [License to inclusion and publication of a Bachelor or Master thesis in the Leiden University Student Repository](#)

Downloaded from: <https://hdl.handle.net/1887/3676806>

**Note:** To cite this publication please use the final published version (if applicable).

---

---

# Studying measures for interpersonal synchrony in brain response by means of applying graph theory measures to EEG data

Martial T.J. Foegel (s2621908)

Thesis advisor: Dr. Tom F. Wilderjans

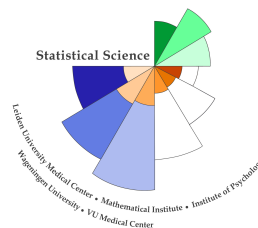
Thesis supervisor: Sophie C. F. Hendrikse

MASTER THESIS

Defended in April 2022



Universiteit  
Leiden



STATISTICS AND DATA SCIENCE

---

---



# Foreword

This thesis was written as part of the master program of Statistical and Data Sciences of Leiden University. It focuses on the detection of interpersonal synchrony in EEG data. In this thesis we use insights from complex network analysis methods to determine which graph theory measures are most appropriate to detect changes in the level of interpersonal synchrony. This thesis is part of a larger project on interpersonal synchrony led by Prof. Sander L. Koole, in collaboration with Dr. Tom F. Wilderjans.

This project was challenging, but highly rewarding. It allowed me to delve back into complex network methods that I studied before and to create an extensive and complex simulation study to answer the research question(s). This was not a one-man job though, and the help of my two supervisors, Dr. Tom F. Wilderjans and Sophie C. F. Hendrikse, was invaluable to the completion of this project.

I would like to thank both of my supervisors for their help during this project. Thanks to you I felt comfortable discussing the different problems encountered along the way and coming up with creative solutions. I would also like to thank you for being understanding whenever I was having difficulties, and for putting my focus back into the question at hand whenever I lost myself down a rabbit hole.

I would also like to extend my thanks to my friends, both in the Netherlands and back in France, who kept me motivated to work on the thesis during this global health crisis. Finally, I would like to thank my family for their support and understanding.

# Table of Contents

<b>Foreword</b>	<b>3</b>
<b>Table of Contents</b>	<b>4</b>
<b>Abstract</b>	<b>5</b>
<b>1 Introduction</b>	<b>9</b>
1.1 Interpersonal Synchrony . . . . .	10
1.2 Graph Theory and Complex Network . . . . .	11
1.3 Research aims . . . . .	14
<b>2 Method</b>	<b>17</b>
2.1 Data . . . . .	17
2.2 Transform functions . . . . .	17
2.2.1 Pearson’s correlation coefficient . . . . .	18
2.2.2 Partial correlation coefficient . . . . .	18
2.2.3 Circular correlation coefficient . . . . .	19
2.2.4 Coherence . . . . .	19
2.3 Complex network topology and graph theory measures . . . . .	19
2.3.1 Unweighted networks . . . . .	20
2.3.2 Weighted networks . . . . .	22
2.3.3 Bipartite networks . . . . .	23
2.3.4 Multiplex networks . . . . .	25
2.3.5 Temporal networks . . . . .	27
<b>3 Simulation</b>	<b>29</b>

3.1	Simulate pairs of EEG data . . . . .	29
3.2	Transform the data to accommodate for Graph Theory measures . . . . .	32
3.3	Accommodating for different network topologies . . . . .	33
3.4	Applying complex network measures . . . . .	34
3.5	Simulation design . . . . .	35
3.6	Statistical Analysis . . . . .	35
3.7	Software . . . . .	37
<b>4</b>	<b>Results</b>	<b>39</b>
4.1	Performance of the different graph theory measures . . . . .	39
4.2	Influence of design factors . . . . .	45
<b>5</b>	<b>Discussion</b>	<b>51</b>
5.1	Main results . . . . .	51
5.2	Limitations and future research . . . . .	53
5.3	Concluding remarks . . . . .	54
	<b>Bibliography</b>	<b>54</b>
	<b>Appendices</b>	<b>60</b>
A	Correlation between graph theory measures . . . . .	61
B	Summary tables with signed correlation . . . . .	62
C	Mixed model ANOVA . . . . .	67
D	Mixed model ANOVA 2 . . . . .	71



# Abstract

In neuroscience, recent research has seen the rise of complex network analysis methods to study brain data from methods like EEG and fMRI. Among the many applications of complex network analysis, it has been used to the study of interpersonal synchrony in brain data (Müller and Lindenberger, 2014; Müller et al., 2013; Sängler et al., 2012). However, the use of complex network analysis in this context is very limited, despite its high potential. To bridge this gap, in this thesis, we present a simulation study allowing for a systematic comparison of the ability of various network analysis measures to capture synchrony and this in the context of different input parameters, functions to transform the data to be suited for network analysis and different types of networks (topology). The results made clear that a lot of graph theory measures, mostly from weighted and unweighted networks, were able to pick up on changes in synchrony. The results also showed the importance of lengthier EEG recordings, as that improved a lot the performance of several graph theory measures. Moreover, the use of Pearson's correlation and circular correlation for transforming the data for network analysis appears to be a better choice than using some other transform functions. Although further research must be done in the field of complex network measures for synchrony, the results are promising for the use of graph theory measures to detect changes in interpersonal synchrony.



# Introduction

Neuroscience is a field of study focusing on the nervous system development, structure, function and degeneration. One of the aims of neuroscience is to study functional connectivity, the connection between brain regions sharing some functional properties. The coordination between those spatially distant brain regions allows for cognitive, psychological and behavioral functions to emerge, and their failings often results in major dysfunction (see Zhang et al., 2021). One way to study the connectivity patterns between brain regions is to use complex network analysis, where brain regions are viewed as vertices, and edges denotes links between these regions. In order to apply such an analysis, we need first some data pertaining to the brain activity. The Electro-Encephalogram (EEG) measures the electrical activity during a given period of time through electrodes placed on the scalp of participants. This allows scientists to gather data of a high temporal accuracy, but with a low spatial precision. On the other hand, the functional Magnetic Resonance Imaging (fMRI) measures oxygenated blood level linked to neuronal activity. This is done using a purposefully built giant magnetic field, allowing for a high spatial precision with a low temporal accuracy. Those two measuring tools are extensively used in the field of neuroscience (Kwong et al., 1992; Szűcs and Csépe, 2004; Yang et al., 2016). Using the data gathered from both the EEG and the fMRI, we can apply complex network analysis, gaining new insight into the brain topology and functionality.

In the case of an EEG, each electrode can be seen as a vertex (Sänger et al., 2012) and for the fMRI, each voxel or Region Of Interest (ROI) can be interpreted as a vertex (Thompson et al., 2017). By formatting the data this way, insight from graph theory, the study of mathematical structures modelling relations between objects, can be gained on those newly dubbed brain networks. Among other things, graph theory is seen as a promising tool to better understand complex inter-brain relations (Czeszumski et al., 2020).

One of such complex inter-brain relations is synchrony. The most basic definition of synchrony is the state of two or more events occurring at the same time. However, when it comes to

behavioural synchrony, temporal regularity is not the sole factor influencing it. Four factors are noted in a recent literature review by Hoehl et al. (2021), namely signal modality, signal emotion, stimulus complexity and the agent being real or virtual. Behavioural synchrony can be observed through a wide range of modalities like movement, language or emotion (Joo et al., 2018; Koole and Tschacher, 2016; Yun et al., 2012), but of particular interest to us is brain synchrony (Seraj, 2018). Synchrony has been scarcely studied through the lens of complex networks, and not much work is done regarding identifying network measures that are able to capture synchrony. As such, we aim to study, by means of a simulation study, how different network measures are affected by changes in synchrony, in order to determine which network measures best capture synchrony.

## 1.1 Interpersonal Synchrony

Interpersonal synchrony occurs whenever the interaction of two or more people gives rise to synchronous actions, meaning that, for instance, these actions may occur at the same time or develop at a similar speed. For this to happen, both a temporal regularity must be put in place as well as the intention behind it understood. Only then can the nervous system pick up on it and consciously or not follow through with a synchronization of one or multiple modalities (Hoehl et al., 2021). The list of modalities this synchrony can be applied to is quite extensive. For example, an experiment by Yun et al. (2012) has shown that a cooperative interaction between two participants increased the synchrony of both fingertip movements and neural activity. During psychotherapy, empirical evidence has been shown to support the fact that movement synchrony, the emergence of a common language, affective coregulation and vocal pitch synchrony support the formation of the therapeutic alliance between patient and psychotherapist (Koole and Tschacher, 2016). It has also been shown that interpersonal synchrony can affect physiological measures such as the respiratory sinus arrhythmia (RSA), i.e., the heart rate variability depending on the phase of respiration (Liu et al., 2018), and that a steady beat can improve the coordination of a group walking together as well as improve inter-subject neural synchrony (Ikeda et al., 2017). Moreover, models have been made of synchrony as emerging from a lower-level element into higher-order mental processes and structure (Nowak et al., 2017).

In general, studying synchrony is beneficial as higher synchrony levels have been linked to more pro-social behaviour in infants (Cirelli et al., 2014), improved group cohesion (Wiltermuth and Heath, 2009) and feelings of being an integral part of a community (Konvalinka et al., 2011). Interpersonal synchrony also facilitates the prediction of a partner's movement, allows a

communicative benefit by reducing cognitive load and much more (Hoehl et al., 2021).

With regards to neural synchrony, this particular brand of interpersonal synchrony has been studied using a method called hyperscanning, meaning that the brain activity of multiple participants is registered at the same time to allow the investigation of intra- and inter-brain relations and synchronization (Burgess, 2013; Czeszumski et al., 2020). For this purpose, EEG data has been used a lot, thanks to the optimal time resolution it permits. In the literature, multiple measures have been applied on pairs of EEG time series to detect synchrony, such as the cross-correlation coefficient, the coherence, the Granger causality and many more (Dauwels et al., 2010). In our case we will apply some of the simpler methods to transform the time series of two subjects into a network representation, after which we will apply a range of graph theory measures to capture synchrony using complex network analysis.

## 1.2 Graph Theory and Complex Network

Complex network analysis has been applied to a vast number of fields, as highly complex systems are present everywhere around us. In social sciences, complex network analysis has put some statement to fame like “there is six degrees of separation between any two individuals” (Travers and Milgram, 1969) or “your friends have more friends than you” (Feld, 1991). Graph theory has also been used in linguistics to evaluate the linguistic complexity of a language (Piperski, 2014), in biology to study the structure of proteins (Mashaghi et al., 2004) and in many more fields of study (see Adalı and Ortega, 2018).

To explain graph theory and complex network analysis, let us start with an example. The transmission of information between neurons of the nervous system using electrical current and molecular exchange is a highly complex phenomenon. There is no easy way to describe it as it is a self-organised system that is constantly evolving, adapting to its surroundings, and contains no central organizing mind. One way to interpret such a complex system is through a complex network, which allows to identify interaction between interconnected components. A complex network analysis usually consists of three steps: (1) measuring a phenomenon in nature (here the exchange of information in the brain), (2) modelling the phenomenon by choosing the right level of coarse-graining for edges and vertices (here the vertices could be electrodes of an EEG measuring the electrical activity on different location on the scalp), stripping the problem to its simplest form and then formulating it in mathematical terms, and (3) validating the model by reproducing or explaining the observations. Graph theory comes in the second part, when

networks are interpreted as graphs, a mathematical structure made up of vertices (also called nodes or points) and edges (also called links or lines), see the Figure 1 below for an illustration.

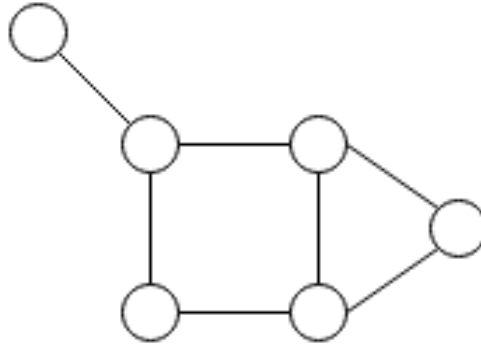


*Figure 1.* Example of a graph with six vertices, represented as circles, and edges connecting some of the vertices.

As we have seen through the example above, the nervous system can be considered as a complex system. As such, in the neuroscience literature, graph theory has been on the rise in recent years. It is used in order to both characterize brain connections as a network (Bullmore and Sporns, 2009; van Wijk et al., 2010) and to study through that framework varied subjects like patient diagnostics of neurological diseases (Naro et al., 2021), epilepsy (Anastasiadou et al., 2019) or the influence of colour on emotion and memory (Chai et al., 2019). Different types of networks have been applied on the brain, like (1) weighted networks (i.e., a network type with weights attributed to the edges) constructed from phase coherence values calculated between pairs of electrodes (Sänger et al., 2012), (2) multiplex networks, where a network is distributed on multiple layers, in order to take into account different frequencies present in EEG data (Buldú and Porter, 2018; Naro et al., 2021) and (3) directed temporal networks (i.e., networks that take into account both the time and the direction of a signal) to differentiate the firing pattern between healthy and Autistic Spectrum Disorder children (Ghahari et al., 2020).

So, we have established that complex networks on the nervous system to study different behavioural phenomena are applied increasingly, but what about synchrony? Well, the studies using graph theory to investigate synchrony are few and far between. Sänger et al. (2012) recorded simultaneous EEG measures of 12 guitar duets. They used intra- and inter-brain phase coherence, representing the degree of phase consistency between two electrodes, to construct a symmetrical coherence matrix. They used that coherence matrix to create a hyperbrain network, meaning a network containing both participants' electrodes, which allows to study both intra-

and inter-brain connections/interactions. From that, they deduced both two within (i.e., one for each subject) and one between brain network, and applied on all four networks (viz., the hyperbrain network, the between network and the two within networks) different graph theory measures. Since they used weighted networks (meaning the edges have an associated weight), they calculated the following measures: (1) the strength (the sum of weighted connections to a node), (2) the clustering coefficient (fraction of neighbours of a node that are linked), (3) the characteristic path length (the average shortest path length between all pairs of nodes), (4) the smallworld coefficient (characterized by both a low characteristic path length and a high clustering coefficient), and (5) the modularity (how much can the network be subdivided into non-overlapping groups). From these measures, they observed that during synchronized play, the smallworld coefficient was increased in the within and hyperbrain network, and that community structure overlapping both brains appeared in the hyperbrain network.

The study by Müller et al. (2013) built on the previous one and had three aims: (1) get the general properties of the brain network, (2) explore different contributions of the within, between and hyperbrain network with different frequencies and (3) check if different roles (both participants playing or one playing and one listening) would map to different network properties. Using the Phase Synchrony Index (a similar measure to the phase coherence but measuring phase stability across time) to construct the network, they applied similar graph theory measures as Sängler et al. (2012). They found that interbrain connections were more obvious at lower frequencies and that sometimes hyperbrain modules appeared, meaning that a community structure overlapping both brains would appear.

In a later work, Müller and Lindenberger (2014) used cross-frequency coupling on phase coherence metrics (meaning they now consider the interaction between frequency bands) to create the now familiar quartet of networks once again. This time it was not used on musical tasks but on couples kissing in different conditions: the partners kissing each other, kissing their own hand or kissing each other while performing a silent arithmetic task. This study revealed a correlation between kissing satisfaction and greater strength and shorter path length when participants kissed each other compared to kissing their own hands.

As we have seen in those three articles, similar graph theory measures have been applied to study synchrony. However, those were always applied on a weighted network based on different transform functions (phase coherence, phase synchrony index, etc.)<sup>1</sup>. No systematic comparison

---

<sup>1</sup>To be more precise, those transform functions are generally referred to as synchrony measures (see for example Seraj (2018)). For the study of graph theory measures themselves, those synchrony measures serve only as a mean to transform the EGG or fMRI data in a format compatible for complex network analysis. As such,

between the transform functions were made, nor between the different graph theory measures applied. Moreover, only the weighted network topology was applied whereas other network topologies have been employed on brain networks and could be relevant. As such, a more extensive study of the use of graph theory measures to characterize synchrony is warranted.

### 1.3 Research aims

Throughout this introduction, we have seen those different types of transform functions have been used to ascertain interpersonal brain synchrony. We have also found out that different network topologies and graph theory measures have been applied to investigate various aspects of EEG data. However, the literature combining the two is very sparse, as only a weighted network topology was applied on differently transformed data. No systematic comparison between those transform functions was made when it comes to using them for complex network analysis. It is, for example, not known which network measures are most suited for quantifying synchrony. Along similar lines, no research has been done investigating the effect of different input parameters (e.g., the number of electrodes or the length of the experiment/time series) on the appropriateness of network measures for capturing synchrony. Also, since only one network topology was applied to study synchrony, one can wonder if other network topologies may be better suited for modeling synchrony. Some of those network topologies have already been applied to study other behavioural phenomena like the temporal and the multiplex networks, but other topologies have not been studied in this context, like the unweighted and the bipartite networks.

Therefore, we propose here to perform a simulation study allowing the systematic comparison between transform functions, different network topologies and their associated graph theory measures, as well as to study the effect of varying input parameters (i.e., data characteristics).

Running this simulation, we expect some of the input parameters to have more impact than others. An obvious example would be the number of electrodes, as this parameter will affect graph theory measures, like degree and strength, that are directly linked to the number of neighbours a given node has. Another parameter, interpersonal synchrony, has already been found by research to have a large effect: performing activities associated with higher interpersonal synchrony has been linked to increases in small-world coefficients, average strength and shorter path length (Müller and Lindenberger, 2014; Müller et al., 2013; Sängner et al., 2012). Concerning transform

---

we will refer to those synchrony measures as transform functions for the rest of this thesis, to avoid any confusion with interpersonal synchrony.

---

function, according to Dauwels et al. (2010), linear measures should give similar results, which should be different from circular measures that consider the circular aspect of EEG. As for network topology, we expect topologies retaining the most information to perform better. In that sense, a weighted network should perform better than an unweighted one as it retains the strength of the connections between the electrodes. A bipartite network should perform slightly worse as it does not consider the connection inside each set of nodes. For the temporal and multiplex network their performance will depend on respectively the temporal dimension and the interlayer information being conserved for their graph theory measures.



# Method

## 2.1 Data

The first step of the simulation is to create EEG data. EEG data records electrical activities across time depending on the number of electrodes placed on the scalp of an individual. Thus, the recording of each electrode is a time series. Here we are interested in the synchrony between two participants, so we have two sets of electrodes. Pairing any two time series forms a dyad, whether those are from the same or different individuals. We end up with as many dyads as there are pairs of electrodes within and between the two participants, and we will apply a transform function on each dyad.

## 2.2 Transform functions

To get from an EEG dataset to an adjacency matrix usable for complex network analysis, a transformation of the data must be done. One possibility in this regard consists of applying a function to each pair of electrodes. For the sake of the computation time of our simulation, we will stick to rather simple functions, like correlation coefficients and coherence. An example is shown in Figure 2.

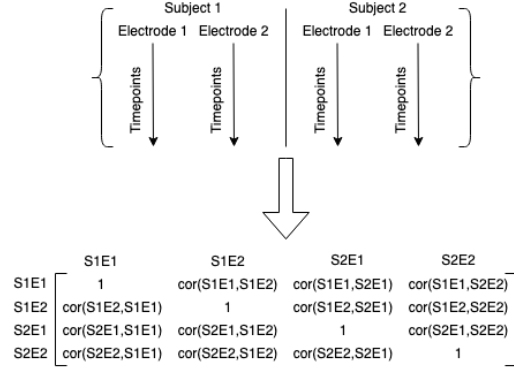


Figure 2. Example of a transformation of an EEG time series using Pearson's correlation coefficient, with S1E1 corresponding to the first electrode (E1) of the first subject(S1), etc.

## 2.2.1 Pearson's correlation coefficient

Pearson's correlation coefficient  $\rho_{xy}$  measures the linear correlation between two variables, here  $x$  and  $y$  (i.e., two EEG time series, one for each member of a dyad). It is calculated by taking the covariance of those two variables divided by the square root of the product of their variances, as can be seen in the equation below:

$$\rho_{xy} = \frac{\sum_{i=1}^n (x_i - \bar{x})(y_i - \bar{y})}{\sqrt{\sum_{i=1}^n (x_i - \bar{x})^2} \sqrt{\sum_{i=1}^n (y_i - \bar{y})^2}} \quad (1)$$

## 2.2.2 Partial correlation coefficient

The Partial correlation coefficient  $\rho_{xy|z}$  measures the association between two variables, here two EEG time series, while controlling for other EEG time series. For a single controlled variable  $z$ , with  $\rho_{xy}$  being the regular correlation coefficient between  $x$  and  $y$  (see equation 1), it is defined as follow:

$$\rho_{xy|z} = \frac{\rho_{xy} - \rho_{xz}\rho_{zy}}{\sqrt{1 - \rho_{xz}^2} \sqrt{1 - \rho_{zy}^2}} \quad (2)$$

If there are multiple controlling variable,  $z$  becomes a set of variables  $Z = \{z_1, z_2, \dots, z_n\}$  and  $\rho_{xy|Z}$  is the correlation between the residuals of the regression of  $x$  on  $Z$  and  $y$  on  $Z$ .

### 2.2.3 Circular correlation coefficient

This is similar to Pearson’s correlation coefficient but is adapted to circular data. Since each electrode produce a signal that is oscillatory, the whole dataset is circular. The aim of a circular correlation coefficient is to see if two signals are related by seeing if one signal being in advance of its expected phase impacts the second signal. This is calculated by measuring the circular covariance of the difference between observed and expected phase of the oscillator. The mathematical formula is very similar to equation 1, but this time a sine function has been applied to both variables  $x$  and  $y$  and the deviation from their mean has also undergone a sinusoidal transformation. The equation is presented below:

$$\rho_{circular} = \frac{\sum_{i=1}^n \sin(x_i - \bar{x}) \sin(y_i - \bar{y})}{\sqrt{\sum_{i=1}^n \sin(x_i - \bar{x})^2} \sqrt{\sum_{i=1}^n \sin(y_i - \bar{y})^2}} \quad (3)$$

### 2.2.4 Coherence

Coherence allows to show how close two time waves are on their frequency domain  $f$ . For two variables  $x$  and  $y$ , the crossspectral density (the distribution of power between two signals as a function of frequency  $f$ ) is indicated as  $G_{xy}(f)$ , and the autospectral density of  $x$  and  $y$  as  $G_{xx}(f)$  and  $G_{yy}(f)$ , respectively, with the magnitude of the spectral density denoted as  $|G|$ . The coherence of  $x$  and  $y$  is then given in the definition below:

$$C_{xy}(f) = \frac{|G_{xy}(f)|^2}{G_{xx}(f)G_{yy}(f)} \quad (4)$$

## 2.3 Complex network topology and graph theory measures

In this section, I will define and explain to a greater extent each type of network we will apply to our dataset. All the networks presented will be considered as undirected, meaning that we will not assign a direction to a given edge between two nodes. We will also present the associated network measures that will be applied. Those measures are only a selection of all graph theory measures available and were chosen according to two factors: their availability through packages in R and their potential links to synchrony.

### 2.3.1 Unweighted networks

The most basic topology for a complex network is an unweighted one. In this case only a single edge is allowed between two nodes, without any direction or weight attributed to it. This edge indicates whether the two nodes are connected or not. An example is presented below with 6 edges:

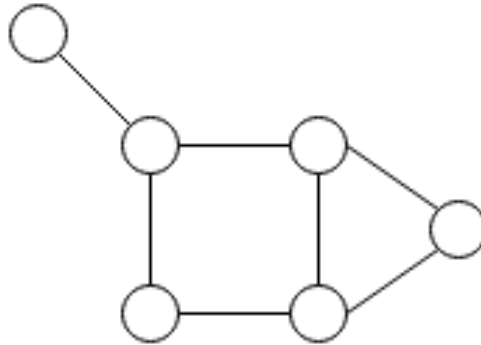


*Figure 3.* Example of a unweighted network. The six nodes represent six electrodes, whereas the edges indicate whether the brain regions corresponding to the electrodes are functionally connected or not.

This type of network can be interpreted as a graph  $G = (V, E)$ , with  $V$  a set of  $N$  vertices  $V = \{v_1, \dots, v_n\}$  (which we will refer to as nodes), and  $E$  a set of edges  $v_i, v_j$  with  $v_i, v_j \in V$  and  $v_i \neq v_j$ . Then, the adjacency matrix  $A$  is a square matrix representing whether an edge is present between two vertices. For example, if the element  $A_{ij} = 1$ , this means there is a connection between vertex  $v_i$  and  $v_j$ . In our case each electrode of both subjects will be considered vertices, forming a hyperbrain network representing both intra and interbrain relations.

The following network measures for unweighted network will be used in this thesis:

- Average degree: the degree of a node is defined as the number of neighbours a given node has. Let us define  $k_i$  as the number of nodes connected to node  $i$ , with  $N$  being the total number of nodes. Then, the average degree is defined as  $\bar{k} = \frac{1}{N} \sum_{i=1}^N k_i$
- Betweenness centrality: the assumption here is that the most important nodes are along the shortest path between two nodes, as information spreads more rapidly along those paths. Let us define  $d_{jk}$ , the shortest path going from node  $j$  to  $k$  and  $d_{jk}(i)$ , the shortest path going from node  $j$  to  $k$  passing through node  $i$ . Then the betweenness centrality of

node  $i$  is defined as follow:  $C_b(i) = \frac{\sum_{jk} d_{jk}(i)}{\sum_{jk} d_{jk}}$ . For our purpose, we will take the average betweenness centrality of all nodes.

- Closeness centrality: it is defined as the inverse of the average shortest distance of a node to all other nodes in the network. The more central a node is, the closer it is to the other nodes. It is defined as:  $C_{cl}(i) = \frac{N-1}{\sum_{d_{ij}<\infty} d_{ij}}$ , with  $d_{ij}$  being the shortest distance between nodes  $i$  and  $j$ . If two nodes are not connected by any path, then by definition the distance between them is infinite, hence the precision  $d_{ij}<\infty$ . For our purpose, we will take the average closeness centrality of all nodes as our metric.
- Characteristic path length: the average number of steps among the shortest paths for all possible pairs of nodes. It is defined as  $\bar{d} = \frac{2}{N(N-1)} \sum_{i<j} d_{ij}$ , with  $d_{ij}$  being the shortest distance between nodes  $i$  and  $j$ .
- Global clustering coefficient: it is a measure of the tendency of nodes to cluster together. Here we use the definition found in Watts and Strogatz (1998) as the average local clustering coefficient. The local clustering coefficient is defined as  $C_u = \frac{2e_u}{k_u(k_u-1)}$ , with  $e_u$  being the number of links between neighbours of node  $u$ , and  $k_u$  the number of neighbour of node  $u$ .
- Modularity: compares edge density in each cluster, given a membership vector indicating the clustering of nodes, to the edge density in a randomized version of the graph. This allows to measure how good the clustering is, or how separated the vertices with different membership are from each other. Here we are using the formula found in Clauset et al. (2004) which goes as follow:  $Q = \frac{1}{2N} \sum_{i,j} \left[ A_{ij} - \frac{k_i k_j}{2N} \right] \delta(c_i, c_j)$ , where  $N$  is the number of edges,  $A_{ij}$  is the element of the  $A$  adjacency matrix in row  $i$  and column  $j$ ,  $k_i$  is the degree of  $i$ ,  $k_j$  is the degree of  $j$ ,  $c_i$  is the type (or component) of  $i$ ,  $c_j$  that of  $j$ . The sum goes over all  $i$  and  $j$  pairs of vertices, and  $\delta(x, y)$  is 1 if  $x = y$  and 0 otherwise.
- Small world coefficient: a coefficient to evaluate how close a network is to being a small world network. A small world network presents clusters of highly interconnected nodes which are highly segregated from other clusters, resulting in very short path lengths. Here the small world coefficient used is the one defined by Humphries and Gurney (2008) as:  $S^{WS} = \frac{\gamma_g^{WS}}{\lambda_g} = \frac{C_g^{WS}/C_{rand}^{WS}}{L_g/L_{rand}}$ , with  $C_g^{WS}$  the Watts-Strogatz clustering coefficient and  $C_{rand}^{WS}$  the corresponding quantity for a random graph,  $L_g$  the mean shortest path length and  $L_{rand}$  the corresponding quantity for a random graph. Values inferior to 3 indicate a small world network.

Since betweenness centrality, closeness centrality and characteristic path length are all graph theory measure of centrality based on the distance between nodes, we expect them to give similar results.

### 2.3.2 Weighted networks

A weighted network is very similar to an unweighted network, with the difference being that weights are attributed to the edges as is illustrated in the figure below (i.e., in the unweighted network the weights are constrained to be zero or one). In our case, weights represent edges strength.

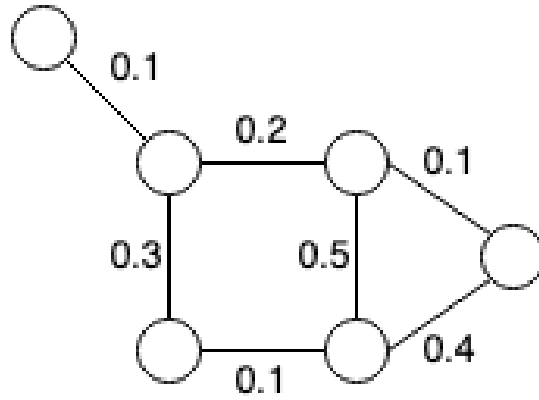


*Figure 4.* Example of a weighted network. The six nodes represent six electrodes, whereas the edges indicate to what extent the brain regions corresponding to the electrodes are functionally connected. This weight could be taken from any of the transform function presented before, like the circular correlation between two electrodes.

The following network measures for weighted network will be used in this thesis:

- Average strength: strength is the sum of the weights of links connected to a given node. For a given node  $i$ , with  $w_{ij}$  being the weight associated with the edge going from  $i$  to  $j$ , then strength is defined as  $\sum_j w_{ij}$ . The average strength is then just averaged over all nodes.
- Betweenness centrality: this is defined similarly as in the unweighted network, except this time, the shortest path is calculated using the inversed edges weight (based on Opsahl et al., 2010).

- Closeness centrality: this is defined similarly as in the unweighted network, except this time, the shortest path is calculated using the inversed edges weight (based on Opsahl et al., 2010).
- Characteristic path length: this is defined similarly as in the unweighted network, except this time, the shortest path is calculated using the inversed edges weight. This is done using Newman and Brandes adaptation to Dijkstra’s algorithm (Brandes, 2001; Newman, 2001).
- Global clustering coefficient: this is an equivalent metric to the unweighted one, but using the weighted version from Onnela et al. (2005):  $\widetilde{C}_i = \frac{2}{k_i(k_i-1)} \sum_{j,k} (\widetilde{w}_{i,j} \widetilde{w}_{j,k} \widetilde{w}_{k,i})^{1/3}$ , with  $\widetilde{w}_{i,j} = w_{i,j} / \max(w_{i,j})$ .
- Modularity: we are using the weighted version of the modularity for unweighted networks presented in Clauset et al. (2004). The main difference being the edge weights are considered as the elements of the adjacency matrix  $A$ , and  $k_i$  is the sum of weights of adjacent edges for vertex  $i$ .
- Small world coefficient: same definition as for unweighted networks, except this one uses the weighted shortest path length and weighted clustering coefficient defined above, similar to what is done for the  $\sigma$  small world coefficient from Müller et al. (2013).

Since betweenness centrality, closeness centrality and characteristic path length are all graph theory measure of centrality based on the distance between nodes, we expect them to give similar results.

### 2.3.3 Bipartite networks

A bipartite graph or a bigraph is a graph whose vertices have been divided between two disjoint independent sets called classes. In our case, if we consider our pair of brains only with regard to their connection between the two participants brains, then we could consider that as a bipartite graph, (i.e., the electrodes of each brain separately form a subset). This bipartite graph is balanced because the two classes have the same number of nodes.

The following network measures for bipartite network will be used in this thesis:

- Average strength: same definition as the one used for weighted networks.
- Betweenness centrality: same definition as the one used for weighted networks.

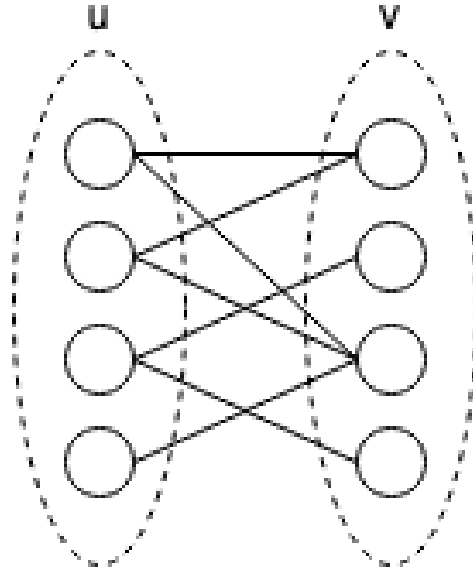


*Figure 5.* Example of a bipartite network in which the electrodes for subject 1 are one class and the electrodes of the second subject constitute the second class. Only links between the electrodes of both brains are modelled in a bipartite graph.

- Cluster coefficient: same definition as the global clustering coefficient used for unweighted networks.
- Nestedness: if a set of neighbours of a node in a class is a subset of neighbours of another node in the same class, we say they are nested. If nestedness is detected in our simulation, it implies a hierarchical structure exists between electrodes of one subject affecting the electrodes of the other subject. If  $B$  is a perfectly nested binary adjacency matrix with  $n$  columns and  $m$  rows, then there exists a permutation of rows and columns such that the set of edges in each row  $i$  contains the edges in row  $i+1$ , while the set of edges in each column  $j$  contains those in column  $j+1$ . To apply this measure to a weighted binary network we will use Weighted Nestedness based on Overlap and Decreasing Fill (WNODF) (Almeida-Neto and Ulrich, 2011). Given our adjacency matrix  $B$ , let  $F$  refer to the number of cells with non-zero values for any column  $c_i$  or row  $r_i$ , where  $i$  indicates column or row position. The weighted value of paired nestedness for any pair of columns is calculated as the percentage of cells in  $c_j$  that have lower values than cells of the same row in  $c_i$ . Then, we can calculate a mean nestedness value for all pairs of columns as:  $WNODFc = 100 \sum_{i=1}^{n-1} \sum_{j=i+1}^n \frac{k_{ij}}{N_j}$ ,

where  $k_{ij}$  denotes the number of cells with lower values in  $c_j$  and  $N_j$  is the total number of non-empty cells in  $c_j$ . Following the same procedure, the value of weighted paired nestedness for any pair of rows is calculated as the percentage of cells in  $r_j$  that have lower values than those cells in  $r_i$  located in the same column positions. Finally, we can calculate the mean paired nestedness for the  $n(n-1)/2$  pairs of columns as well as for the  $m(m-1)/2$  pairs of rows. WNODF can be calculated as:  $\frac{2(WNODFc+WNODFr)}{m(m-1)+n(n-1)}$

- Connectance: the fraction of all possible links realized in the network:  $\frac{L}{N^2}$  with  $L$  the number of links and  $N$  the number of electrodes on one participant. This measure is related to the linkage density (Dunne et al., 2002).

### 2.3.4 Multiplex networks

A multiplex network is a specific type of multilayer network. Both differ from previously mentioned network as they present networks with multiple layers. Meaning that the nodes and edges of this network can exist on one or multiple layers, each layer representing a different mode of interaction (e.g., different coupling frequencies of EEG data or in our case different subjects). Connections between nodes of the same layer are called intralayer connections, and between different layers interlayer connections. A multiplex network is a special case of a multilayer network, where each node is present in each layer. In our case the electrodes of each subject will be considered as vertices with each subject being a layer of the multiplex network.

For a given multiplex network,  $\alpha$  is the layer, with  $M$  the total number of layers and  $N$  the number of nodes (assuming all layers have the same  $N$  nodes). The strength of node  $i$  is defined as a vector  $s_i = (s_i^{[1]}, \dots, s_i^{[M]})$ ,  $i = 1, \dots, N$ . For some measures linked to multiplex network, we work with overlapping edges and nodes, meaning we combine their value by adding them up across layers. As such we can define the weighted overlap of an edge  $i - j$  as  $o_{ij}^w = \sum_{\alpha} w_{ij}^{[\alpha]}$  and the weighted overlapping strength of node  $i$  as  $o_i^w = \sum_j s_i^{[\alpha]}$ .

The following network measures for multiplex network will be used in this thesis:

- Entropy of multiplex degree: measures how homogeneously the nodes are distributed; it takes a value of 0 if all links of a given node are on a single layer and 1 if links are evenly distributed over the different layers. The version presented here is a weighted adaptation of the one found in Battiston et al. (2014). Entropy of node  $i$  is defined as:

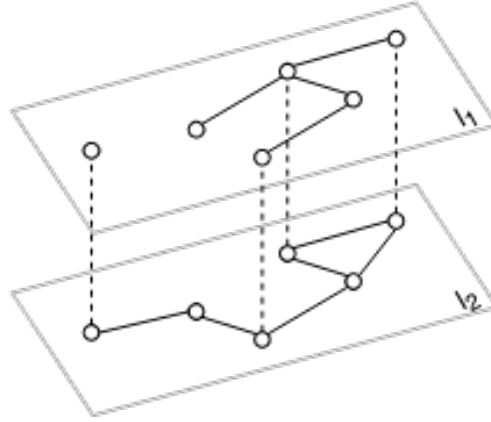


*Figure 6.* Example of a multiplex network. The six nodes in the first layer  $l_1$  represent six electrodes of the first subject and the same six electrodes are present for the second subject ( $l_2$ ). As always, the edges indicate whether the brain regions corresponding to the electrodes are functionally connected or not.

$$H_i = - \sum_{\alpha=1}^M \frac{s_i^{[\alpha]}}{o_i^w} \ln \left( \frac{s_i^{[\alpha]}}{o_i^w} \right)$$

In general, the higher the value of  $H_i$ , the more uniformly the links of node  $i$  are distributed across the layers.

- Degree centrality: this measure captures how important a node is based on the weights of its edges. This is calculated using the formulas in De Domenico et al. (2013). The degree centrality is the sum of the aggregated edges for each node, but using a 1-tensor to represent connections between the two layers, meaning here, we consider each node to be fully connected with itself at different layers.
- Global overlay clustering coefficient: the measure is based on a similar principle as the global clustering coefficient of weighted networks; here, it is adapted for multiplex networks (De Domenico et al., 2013). Meaning it is the average of the local clustering coefficient of the overlay monoplex network obtained from overlapping the layers of the multiplex network. This measure is standardized as to allow for comparison with other multiplex network by dividing it by the maximum value in the overlay adjacency matrix divided by the number of layers.

- Degree correlation: calculates the correlation between degrees of the same node in different layers. In order to do that a simple Pearson correlation coefficient can be used between the adjacency matrices of each layer, as is advocated in Nicosia and Latora (2015).

### 2.3.5 Temporal networks

A temporal network is a network whose edges can change (i.e., be active or inactive or become more or less activated) across time. The problem we run into here is that a neural network is a particular type of time-varying network called an annealed network, meaning the evolution of the network is much faster than the observation. That is why we will here take a snapshot of the network, i.e., averaged over a period of time, and apply some network measures to each snapshot of an unweighted network.

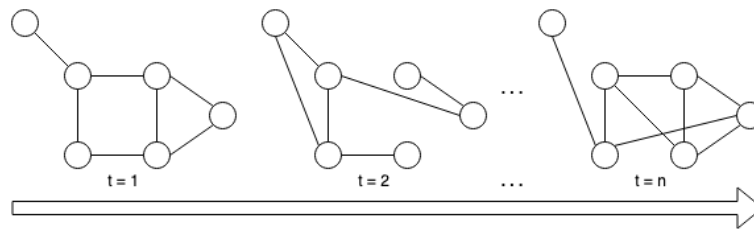


*Figure 7.* Example of a temporal network. Each snapshot of the network can be interpreted as the unweighted network. Adding the time component allows to see which brain regions gain or lose their functional connectivity.

The following network measures for temporal network will be used in this thesis:

- Average degree: defined the same as for the unweighted network.
- Betweenness centrality: defined the same as for the unweighted network.
- Closeness centrality: defined the same as for the unweighted network.
- Density: this measure computes the total duration (or count of events) of activity of all the edges in the network, and divides this by the total amount of observable time for all the possible pairs of nodes. A value of 1 corresponds to a fully connected network in which all edges are always active, whereas a value of 0 indicates a network with no active edges. This measure can be interpreted as the average fraction of possible edges that are active at any time point.

- Edge formation: formation returns the ratio of the number of ties formed to the number of possible empty pairs of nodes that could have formed ties. So, a value of 1 would mean that all empty dyads formed ties, whereas a value of 0 means no ties were formed. In sparse networks, the value will tend to be close to 0, as few ties get formed among the possible pairs of nodes without a tie.
- Average components: average number of components within a given graph across time, i.e., the number of disjoint sets of vertices.

# Simulation

The aim of our simulation is to see which graph theory measure best characterizes changes in synchrony between EEG data of two participants. In order to do that, we will first simulate EEG data with a given interpersonal synchrony value, then transform the data using a selection of transform functions. This will accommodate the data to the format of network analysis, and apart from a few minor modifications linked to the requirement of different network topologies, we can then apply a range of graph theory measures to those networks. Once that is done, we will be able to determine which measure overall, and for each network topology separately, is most associated with change of interpersonal synchrony. We also aim to see if those measures are resistant to change in the simulation parameters, like the number of electrodes and the signal to noise ratio, amongst others.

## 3.1 Simulate pairs of EEG data

In order to create a pair of EEG time series data with a given level of interpersonal synchrony, here referred to as interbrain synchrony, we start from a covariance matrix that includes both the covariance between the electrodes of each participant, and the covariance between the electrodes of different participants. Then, using this covariance matrix, we will use a multivariate normal distribution to simulate the data.

In order to create a covariance matrix, we will be using simple matrix multiplication. The principle is that we create a matrix  $B$  with the first half of the first line and the last half of the second line with a high value. For example, for two electrodes in each brain, the first line will have two high values and then two low values, and it will be the other way around for the second line. This is illustrated below with  $h$  a high value and  $l$  a low one:

$$B = \begin{bmatrix} h & h & l & l \\ l & l & h & h \end{bmatrix} \quad (5)$$

This way, when we create our covariance matrix using  $B^T B$ , the top left and bottom right sub-matrices (i.e., representing intra-brain connections, within the brain of the same subject) will both get high values, and the rest much lower values (i.e., representing inter-brain connections, between regions of different subjects). Note that it is realistic to assume that inter-brain connections are weaker than intra-brain connections. For the above-mentioned matrix  $B$ , this leads to:

$$B^T B = \begin{bmatrix} \begin{pmatrix} h^2 + l^2 & h^2 + l^2 \\ h^2 + l^2 & h^2 + l^2 \end{pmatrix} & \begin{pmatrix} 2hl & 2hl \\ 2hl & 2hl \end{pmatrix} \\ \begin{pmatrix} 2hl & 2hl \\ 2hl & 2hl \end{pmatrix} & \begin{pmatrix} h^2 + l^2 & h^2 + l^2 \\ h^2 + l^2 & h^2 + l^2 \end{pmatrix} \end{bmatrix} \quad (6)$$

We are using the following matrix multiplication  $B^T B$  to ensure a valid covariance matrix, as  $B^T B$  is positive semi-definite if and only if the matrix  $B_{k \times n}$  is of full row rank  $k$  (which is always the case except when  $h = l$ , nothing a simple check could not detect). If we then feed this covariance matrix into the *rmvnorm* of the **mvtnorm** package (Genz et al., 2021), we will get a matrix with 4 columns, the first two corresponding to the first brain and the second half to the second brain. Putting more electrodes just changes the factor in front of  $hl$  and the power of each element of the addition  $h + l$ , as illustrated here with  $n$  electrodes:

$$B^T B_{2n \times 2n} = \begin{bmatrix} (h^n + l^n)_{n \times n} & (nhl)_{n \times n} \\ (nhl)_{n \times n} & (h^n + l^n)_{n \times n} \end{bmatrix} \quad (7)$$

Rather than choosing the  $h$  and  $l$  values at the beginning of the simulation, we can actually choose what we will refer to as the intrabrain and interbrain value, respectively  $y = h^n + l^n$  (for the intrabrain value) and  $x = nhl$  (for the interbrain value). To do that, we can find the  $h$  and  $l$  values by solving the above equations, which results in:

$$l = \sqrt[n]{\frac{y \pm \sqrt{y^2 - \frac{4x^n}{n^n}}}{2}} \quad (8)$$

and  $h = \frac{x}{n \sqrt[n]{\frac{y \pm \sqrt{y^2 - \frac{4x^n}{n^n}}}{2}}}$

For the purpose of our simulation, the intrabrain value will always be defined by adding 0.3 to the interbrain value. If we then use the covariance matrix and apply it to our multivariate normal function, we get, for a given set of parameters with multiple replicates, a data structure like the one depicted below:

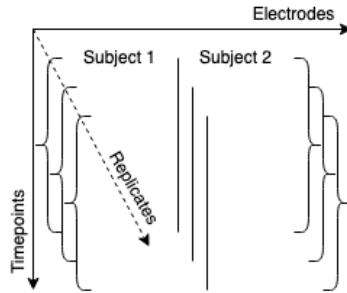


*Figure 8.* Resulting dataset after the first step of the simulation. The sets of electrodes of the two subjects are presented side by side with each electrode (column) being recorded over time (rows). The third dimension, depth, represents the replicates used in the simulation design.

Moreover, for a given set of parameters, some variation can be added between replicates, by slightly changing the interbrain and intrabrain values between each replicate. For this purpose, for each replicate the actual inter- and intrabrain value will be taken from a uniform distribution between the specified value plus or minus .05.

We will also be adding normally distributed noise to the data. This noise will be spatially and temporally autocorrelated to reflect the fact that EEG data is both spatially and temporally correlated. This is done via the function `colored_noise` from the package **colorednoise** (Pilowsky, 2020) which uses this formula  $\epsilon_{t+1} = k\epsilon_t + \omega_t\sqrt{1-k^2}$ , with  $\epsilon_t$  being the autocorrelated variable at time point  $t$ ,  $\omega_t$  the innovation at time point  $t$  for which a standard normal variable is assumed and  $k$  the autocorrelation. For the temporal autocorrelation, we will create a matrix of autocorrelated columns, with each column corresponding to an electrode. As for the spatial autocorrelation, we will create a matrix where each row is autocorrelated for each subject. These two matrices will then be added together, and this total autocorrelated noise matrix will be added to the (true) data. We can tune the amount of signal to noise ratio by multiplying the noise matrix by a given value, which is calculated as  $k = \frac{\sigma_{data}}{SNR \times \sigma_{noise}}$  with  $\sigma_{data}$  being the standard deviation of the data and  $\sigma_{noise}$  the standard deviation of the noise, and  $SNR$  a given signal to noise ratio (Hastie et al., 2009).

To recap, the parameters that we can manipulate so far are both the interbrain and intrabrain

value, the number of timepoints and electrodes, both the spatial and temporal autocorrelation as well as the signal to noise ratio.

### 3.2 Transform the data to accommodate for Graph Theory measures

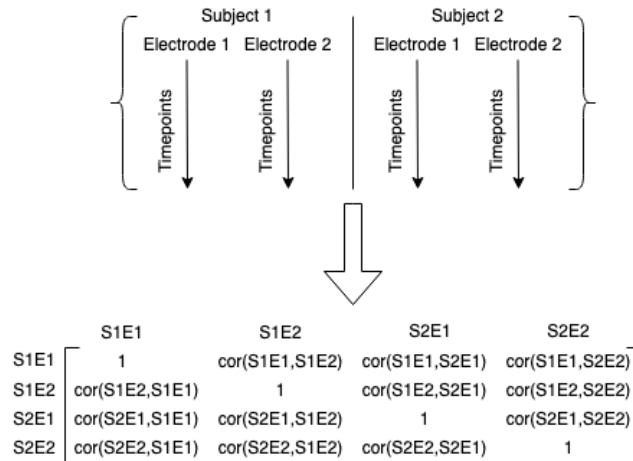
The options to transform the data into a format compatible with graph theory measures are: correlation, partial correlation, circular correlation and coherence (see Table 1 for an overview of the R functions and packages used to perform these transformation).

Table 1

*Summary of all the transform functions applied and their respective R functions, packages and references.*

Transformation measure	R function	R package	Reference
Pearson's correlation coefficient	<i>cor</i>	<b>stats</b>	R Core Team (2020)
Partial correlation	<i>pcor</i>	<b>ppcor</b>	Kim (2015)
Circular correlation	<i>cor.circular</i>	<b>circular</b>	Agostinelli and Lund (2017)
Coherence	<i>coh</i>	<b>seewave</b>	Sueur et al. (2008)

For example, applying Pearson's correlation between each column of our dataset gives back a correlation matrix, which can be directly interpreted as a weighted adjacency matrix. The repartition of said matrix between within and between subject correlation is presented below:



*Figure 9.* Example of a transformation using Pearson's correlation coefficient with with S1E1 corresponding to the first electrode (E1) of the first subject(S1), etc.

### 3.3 Accommodating for different network topologies

The transformation done in the previous step will give back an adjacency matrix which is immediately compatible with weighted network measures. The other network topologies will need some slight adjustments.

For the unweighted network, we needed to binarize the data according to some threshold. To determine this threshold, a permutation testing approach is adopted. The permutations are done by randomly shuffling sets of 10 timepoints of each electrode for the two subjects and reconstructing the adjacency matrix afterwards. This way a given number of permutations are performed and a null distribution is available for each element of the adjacency matrix. Then only the real values above a given threshold of their respective null distribution are retained as 1, otherwise taking the value 0. The alpha value for this threshold will be fixed at 0.01 in order to create a slightly sparser network (Müller and Lindenberger, 2014).

For the bipartite network, we will only take the correlation between the two subjects into account and put each electrode of subject 1 in the first column, each electrode of subject 2 in the second column, and use the weight of the adjacency matrix between the two subjects as the weight for the links between the two columns.

For the multiplex network, we will only consider the correlation within each subject, with each subject being its own layer. This results in a network with two layers capturing the intrabrain connections within each subject. The correlation between subjects is not considered, as no packages in R provide support for including them as interlayer weights (i.e., interbrain connections will not be added as a third layer).

For the temporal network, we will need to transform the data into binary data for different windows of time. Here we will use snapshots of 100 timepoints for each time window (with no overlap between windows). To binarize each of those snapshots, we will not be using the permutation approach presented above for the unweighted network, as it is computationally too intensive. Instead, we will use the *threshold* function from the **NetworkToolbox** package, which uses a false discovery rate methodology to create a threshold. The value used for this threshold is an  $\alpha$  of .05 on a Student's t-distribution (Christensen, 2018).

### 3.4 Applying complex network measures

The measures listed in the method section will be applied on their corresponding network topology, as summarized in Table 2:

Table 2

*Overview of all the measures used during the simulation and the respective R functions and R packages and references.*

Network topology	Measure	R package	Reference
Weighted Network	Average strength	<b>qgraph</b>	Epskamp et al. (2012)
	Betweenness centrality	"	"
	Closeness centrality	"	"
	Characteristic path length	"	"
	Global clustering coefficient	"	"
	Modularity	"	"
	Small world coefficient	Custom made	Adapted from Müller et al. (2013).
Unweighted Network	Average degree	<b>qgraph</b>	Epskamp et al. (2012)
	Betweenness centrality	"	"
	Closeness centrality	"	"
	Characteristic path length	"	"
	Global clustering coefficient	"	"
	Modularity	"	"
	Small world coefficient	Custom made	Humphries and Gurney (2008)
Bipartite Network	Average strength	<b>qgraph</b>	Epskamp et al. (2012)
	Betweenness centrality	"	"
	Cluster coefficient	<b>bipartite</b>	Dormann et al. (2009)
	Nestedness	"	"
	Connectance	"	"
Multiplex Network	Entropy of multiplex degree	Custom made	Weighted adaptation of Battiston et al. (2014)
	Degree centrality	<b>mplex</b>	Degani (2017)
	Global overlay coefficient	"	"
	Degree correlation	Custom made	Adapted from (Nicosia and Latora, 2015)
Temporal Network	Average degree	<b>tsna</b>	Bender-deMoll and Morris (2021)
	Betweenness centrality	"	"
	Closeness centrality	"	"
	Density	"	"
	Edge formation	"	"
	Average component	"	"

### 3.5 Simulation design

The design of the simulation study is presented in Table 3, which shows the factors and its parameters that will be manipulated during our simulation.

Table 3

*Summary of manipulated factors and the parameters used for each factor.*

Manipulated parameter	Values
Number of electrodes	16 / 32
Number of timepoints	1000 / 10000
Spatial autocorrelation	.20 / .60
Temporal autocorrelation	.20 / .60
Signal to noise	1 / 3
Transform function	correlation / partial correlation circular correlation / coherence

The simulation design will have in total 128 conditions (i.e., all possible combinations of the levels of the factors listed in Table 3). For each condition, 10 replicated data sets around each of 3 theoretical interbrain values will be generated (i.e., in total 30 data sets will be generated per condition). On each generated data set, the 29 graph theory measures - coming from 5 different network topologies- will be applied. For the theoretical interbrain value, the following three values will be used: .10 (small synchrony), .50 (medium synchrony) and .90 (large synchrony).

Some of the parameters of the simulation will be kept fixed. This simulation will only use two subjects, with the intrabrain value always being .30 above the generated interbrain value. In order to create unweighted networks, the binarization parameter (i.e., threshold) will be based on 100 permutations and an alpha value of .01. For temporal networks, the size of the snapshots for temporal networks will be 100 timepoints (meaning we have 10 and 100 snapshots when using 1000 and 10000 timepoints, respectively). Finally, to calculate the smallworld coefficient for both weighed and unweighted networks, 20 corresponding random networks will be used.

### 3.6 Statistical Analysis

In total, 3840 data sets are generated (i.e., 10 replicates around each of 3 theoretical interbrain values for each of the 128 simulation conditions). For each generated data set, a true synchrony value will be defined and estimates for synchrony will be provided based on each of the 29 considered graph theory measures (See Table 2). As definition for true synchrony, we will use

the interbrain value. Note that the actual interbrain value used for each data set is sampled at random from a uniform distribution with range .10 around the theoretical interbrain value, which is manipulated as .10 (small), .50 (medium) or .90 (large synchrony).

For 90 data sets, however, no value could be estimated for the closeness centrality measure from the unweighted network; for these data sets, the characteristic path length of the unweighted network was also marked as infinite. This appeared to happen whenever the threshold used for the network created a network that was too sparse. When this was the case, one or more components (i.e., groups of interconnected nodes) were unconnected to the rest of the network. By convention, the path length between members of two unconnected components is considered to be infinite and thus not included in both the closeness centrality and characteristic path length metric. As such, those 90 results for both metrics were excluded from the rest of the analysis.

The goal of our analysis is to find links between synchrony and the different graph theory measures. In order to do so, we computed the correlation between the interbrain value (true synchrony) and the different graph theory measures. This correlation is computed across the 30 data sets (i.e., three interbrain values and ten replicates for each value) (and across snapshots for temporal network measures) within each cell of the design (see Table 3). Note that we do not calculate the Mean Squared Error (MSE) between the true and estimated synchrony value as the different graph theory measures are expressed on different scales, which makes it senseless to check whether the obtained measures equal the true interbrain value. Some of the correlations, however, could not be calculated as there was no variance for a few graph theory measures for some cells of the simulation design. This will only slightly impair the presentation of the performances of each graph theory measure, but is detrimental to the analysis of the effect of the design factors. To simplify further analysis of the design factors, therefore, the graph theory measures yielding any missing values were removed. This way, we discarded the following five graph theory measures from the analysis: (1) betweenness centrality for weighted networks, (2) betweenness centrality for bipartite networks, (3) connectance, (4) cluster coefficient and (5) weighted nestedness for bipartite networks. This results in 24 graph theory measures left for the analysis.

To guarantee a proper analysis down the line, we took the absolute value of the correlation between the (true) interbrain value and the estimated graph theory measure. This is done to ensure that all graph theory measures properly could be compared to each other in terms of performance, as for some graph theory measures a larger interbrain value will result in a smaller graph theory measure value. For example, the more connected a graph is (which could be

considered as a sign of more synchrony between the network nodes), the shorter the characteristic path length of the network is.

In order to analyze our data, we will use a mixed model ANOVA, with both between and within variables. This is because some (between) factors are different between each simulated dataset (i.e., the number of electrodes and timepoints, the spatial and temporal autocorrelations, and the signal to noise ratio), whilst other (within) factors were applied on the same data set (i.e., the method used to transform the data and the graph theory measure computed). Because we have a single datapoint (correlation) in each design cell, we will not include the highest order interaction in the analysis of the effect of the factors on performance. When, in this analysis, some factors are not involved in any important main and/or interaction effect, we will exclude these factors from the ANOVA and present the results, also fitting the highest order interaction (which is possible now because there are multiple data points per design cell).

In order to satisfy the model assumptions for mixed model ANOVA, we transformed the response variable using the Fisher z-transform. For simplicity of interpretation, the figures will be presented without said transformation. After the transformation of the response variable, we confirmed that both the normality and independence assumptions were met. The sphericity of the covariance matrix assumption however, was not met. Hence, we used the Greenhouse–Geisser adjustment for the p-values (Geisser and Greenhouse, 1958). The mixed ANOVA will be fitted using the *Anova* function from the **car** package (Fox and Weisberg, 2019). As in a simulation study, due to the large sample size, most effects are significant at  $\alpha = .05$ , we will also compute effect sizes to determine the most important (main and interaction) effects. The effect sizes will be calculated according to the recommendations by Bakeman (2005) for mixed model ANOVAs.

### 3.7 Software

This work was performed using the computing resources from the Academic Leiden Interdisciplinary Cluster Environment (ALICE) provided by Leiden University. All the code for both the simulation and the statistical analysis are available at <https://github.com/Manitou68/Master-Thesis.git>.



# Results

## 4.1 Performance of the different graph theory measures

For the unweighted network, the mean absolute correlation (standard deviation between parenthesis) for each graph theory measure for each level of the manipulated factors is displayed in Table 4. In this table, one can see that overall the best performing graph theory measure is the closeness centrality (with a mean correlation of .47), closely followed by the average degree, the betweenness centrality, characteristic path length (.46) and the modularity (.45). The similar results of these graph theory measures can be explained by the strong correlation present between them (see Appendix A). The small world coefficient (.40) and the global clustering coefficient (.34) perform a bit worse. Note the quite large standard deviations in performance. It appears that this pattern of results is similar no matter the number of electrodes, number of timepoints, signal to noise ratio, and amount of temporal or spatial autocorrelation. For the transform function, however, the difference between the best and worst performing methods is way larger when using Pearson’s correlation and circular correlation as compared to using partial correlation or coherence. Indeed, for the latter two transform functions, there are almost no performance differences between the methods. Remarkably, the average degree (slightly) performed the best when using partial correlation. In general, for all measures, performance is clearly better when using Pearson’s and circular correlation than when adopting coherence and partial correlation. Also having more time points and less electrodes seems to improve the performance, with the other manipulated factors having no large influence on performance.

For the second type of network, weighted networks, results are presented in Table 5. The results show that the global clustering coefficient (mean correlation of .50) performed better overall, slightly ahead of the average strength (.48), the closeness centrality (.47) and the characteristic path length (.46). A bad performance was observed for the betweenness centrality (.28), with an intermediate performance for the modularity and small world coefficient (.43 and .42

Table 4

*Average absolute correlation overall and for each level of the manipulated factors (and corresponding standard deviation between parenthesis) for each graph theory measure from unweighted networks.*

	Clos. centr.	Avg. degree	Betw. centr.	Charac. path length	Modul.	Small world coef.	Global clust. coef.	Overall
16 electrodes	<i>0.52</i> (0.31)	0.51 (0.31)	0.51 (0.30)	0.51 (0.30)	0.51 (0.31)	0.47 (0.31)	0.42 (0.23)	0.49 (0.30)
32 electrodes	<i>0.41</i> (0.32)	0.40 (0.31)	<i>0.41</i> (0.32)	<i>0.41</i> (0.32)	0.40 (0.32)	0.34 (0.33)	0.25 (0.20)	0.37 (0.30)
1000 time points	0.37 (0.25)	0.34 (0.23)	<i>0.38</i> (0.25)	<i>0.38</i> (0.25)	0.35 (0.25)	0.29 (0.24)	0.33 (0.21)	0.35 (0.24)
10000 time points	0.56 (0.35)	<i>0.57</i> (0.34)	0.55 (0.34)	0.55 (0.34)	0.55 (0.35)	0.52 (0.35)	0.35 (0.25)	0.52 (0.33)
Ac. temp. of 0.2	<i>0.46</i> (0.32)	0.44 (0.32)	0.45 (0.32)	0.45 (0.32)	0.44 (0.33)	0.40 (0.32)	0.33 (0.23)	0.42 (0.31)
Ac. temp. of 0.6	<i>0.48</i> (0.31)	0.47 (0.30)	<i>0.48</i> (0.31)	<i>0.48</i> (0.31)	0.47 (0.31)	0.41 (0.33)	0.35 (0.24)	0.45 (0.30)
Ac. spatial of 0.2	<i>0.48</i> (0.30)	0.45 (0.31)	0.47 (0.30)	0.47 (0.30)	0.46 (0.31)	0.41 (0.32)	0.34 (0.21)	0.44 (0.29)
Ac. spatial of 0.6	<i>0.46</i> (0.33)	<i>0.46</i> (0.32)	<i>0.46</i> (0.33)	<i>0.46</i> (0.33)	0.45 (0.33)	0.40 (0.33)	0.34 (0.25)	0.43 (0.32)
SNR of 1	<i>0.46</i> (0.33)	0.45 (0.32)	<i>0.46</i> (0.32)	<i>0.46</i> (0.32)	0.44 (0.33)	0.40 (0.33)	0.37 (0.24)	0.43 (0.31)
SNR of 3	<i>0.48</i> (0.31)	0.47 (0.31)	0.47 (0.30)	0.47 (0.30)	0.47 (0.31)	0.41 (0.32)	0.30 (0.22)	0.44 (0.30)
Pearsons cor.	<i>0.73</i> (0.22)	0.69 (0.25)	0.72 (0.21)	0.72 (0.21)	0.70 (0.24)	0.64 (0.29)	0.47 (0.24)	0.67 (0.24)
Partial cor.	0.15 (0.10)	<i>0.17</i> (0.12)	0.16 (0.10)	0.16 (0.10)	0.13 (0.11)	0.14 (0.11)	0.13 (0.10)	0.15 (0.11)
Circular cor.	<i>0.74</i> (0.20)	0.71 (0.22)	0.73 (0.19)	0.73 (0.19)	0.72 (0.21)	0.65 (0.28)	0.49 (0.20)	0.68 (0.21)
Coherence	0.25 (0.14)	0.25 (0.14)	0.25 (0.14)	0.25 (0.14)	0.25 (0.15)	0.18 (0.10)	<i>0.26</i> (0.15)	0.24 (0.14)
Global average <sup>1</sup>	<b>.47</b> (0.32)	0.46 (0.31)	0.46 (0.31)	0.46 (0.31)	0.45 (0.32)	0.40 (0.32)	0.34 (0.23)	0.43 (0.30)

*Note.* In italic are the best performing measures for each level of the manipulated factor. In bold is the best performing measure across all manipulated factors.

<sup>1</sup> Corresponds to an average across all manipulated factors

respectively). This pattern of results is similar across the levels of the number of timepoints and electrodes, the signal to noise ratio and the (spatial and temporal) amount of autocorrelation. For the transform function, the only exception is the partial correlation for which the modularity and the average strength performed slightly better than the other measures. Again, as in Table

4 performance is better with more time points and less electrodes and for the Pearson's and circular correlation.

Table 5

*Average absolute correlation overall and for each level of the manipulated factors (and corresponding standard deviation between parenthesis) for each graph theory measure from weighted networks.*

	Global clust. coef.	Avg. strength	Clos. centr.	Charac. path length	Modul.	Small world coef.	Betw. centr.	Overall
16 electrodes	<i>0.54</i> (0.36)	0.52 (0.36)	0.53 (0.33)	0.52 (0.31)	0.47 (0.34)	0.45 (0.33)	0.34 (0.23)	0.48 (0.32)
32 electrodes	<i>0.45</i> (0.32)	0.44 (0.31)	0.40 (0.29)	0.39 (0.28)	0.39 (0.28)	0.38 (0.26)	0.21 (0.16)	0.38 (0.27)
1000 time points	<i>0.38</i> (0.27)	0.35 (0.27)	<i>0.38</i> (0.25)	0.37 (0.25)	0.30 (0.22)	0.37 (0.25)	0.26 (0.21)	0.34 (0.25)
10000 time points	<i>0.61</i> (0.37)	0.60 (0.35)	0.56 (0.35)	0.54 (0.33)	0.56 (0.34)	0.46 (0.33)	0.30 (0.21)	0.52 (0.33)
Ac. temp. of 0.2	<i>0.48</i> (0.34)	0.46 (0.34)	0.46 (0.31)	0.45 (0.30)	0.45 (0.31)	0.43 (0.30)	0.27 (0.21)	0.43 (0.30)
Ac. temp. of 0.6	<i>0.51</i> (0.35)	0.50 (0.33)	0.47 (0.33)	0.46 (0.31)	0.41 (0.32)	0.40 (0.30)	0.29 (0.21)	0.43 (0.31)
Ac. spatial of 0.2	<i>0.49</i> (0.36)	<i>0.49</i> (0.35)	0.48 (0.32)	0.46 (0.30)	0.46 (0.31)	0.46 (0.31)	0.33 (0.23)	0.45 (0.31)
Ac. spatial of 0.6	<i>0.50</i> (0.33)	0.47 (0.33)	0.46 (0.32)	0.45 (0.31)	0.40 (0.32)	0.37 (0.29)	0.21 (0.16)	0.41 (0.29)
SNR of 1	<i>0.49</i> (0.35)	0.48 (0.34)	0.45 (0.30)	0.45 (0.29)	0.39 (0.30)	0.35 (0.26)	0.24 (0.16)	0.41 (0.29)
SNR of 3	<i>0.50</i> (0.34)	0.47 (0.34)	0.48 (0.34)	0.47 (0.32)	0.46 (0.32)	0.48 (0.32)	0.32 (0.25)	0.45 (0.32)
Pearsons cor.	<i>0.75</i> (0.25)	0.69 (0.31)	0.70 (0.23)	0.68 (0.22)	0.65 (0.27)	0.59 (0.27)	0.38 (0.19)	0.63 (0.25)
Partial cor.	0.13 (0.11)	0.15 (0.09)	0.12 (0.09)	0.12 (0.10)	<i>0.17</i> (0.12)	0.14 (0.11)	0.09 (0.07)	0.13 (0.10)
Circular cor.	<i>0.75</i> (0.24)	0.69 (0.27)	0.71 (0.20)	0.69 (0.18)	0.64 (0.29)	0.61 (0.26)	0.39 (0.18)	0.64 (0.23)
Coherence	0.36 (0.25)	<i>0.38</i> (0.26)	0.33 (0.23)	0.33 (0.23)	0.25 (0.19)	0.33 (0.24)	-	0.33 (0.23)
Global average <sup>1</sup>	<b>0.50</b> (0.34)	0.48 (0.34)	0.47 (0.32)	0.46 (0.30)	0.43 (0.31)	0.42 (0.30)	0.28 (0.21)	0.43 (0.30)

*Note.* In italic are the best performing measures for each level of the manipulated factor. In bold is the best performing measure across all manipulated factors. The case with a dash correspond to particular combination of factors where for all data sets of that design cell the graph theory measures had no variance and thus the correlation was not defined.

<sup>1</sup> Corresponds to an average across all manipulated factors

The results for bipartite networks are presented in Table 6. The graph measures with the largest correlation are the average strength (.48) and the connectance (.47), closely followed by the cluster coefficient (.44) and the nestedness (.43). The betweenness centrality gave a bad performance (.28). This trend was observed regardless of the amount of autocorrelation (both for temporal and spatial) and when using the Pearson and circular correlation as transform function (although for these two transform functions, the average degree outperformed the other measures to a stronger degree compared to overall). For 16 electrodes, 1000 timepoints and an SNR of 3, the average strength performed better than the other methods, whereas for 32 electrodes, 10000 timepoints, SNR equalling 1 and the partial correlation, the connectance was the best performing method. The main effects of the factors showed similar patterns as in the previous tables.

Table 6

*Average absolute correlation overall and for each level of the manipulated factors (and corresponding standard deviation between parenthesis) for each graph theory measure from bipartite networks.*

	Avg. strength	Connect.	Cluster coef.	Nestedness	Betw. centr.	Overall
16 electrodes	<i>0.52</i> (0.36)	0.47 (0.25)	0.44 (0.23)	0.47 (0.28)	0.34 (0.23)	0.45 (0.27)
32 electrodes	0.44 (0.31)	<i>0.46</i> (0.24)	0.44 (0.22)	0.39 (0.32)	0.21 (0.16)	0.39 (0.25)
1000 time points	0.35 (0.27)	<i>0.44</i> (0.25)	0.42 (0.24)	0.31 (0.23)	0.26 (0.21)	0.36 (0.24)
10000 time points	<i>0.60</i> (0.35)	0.49 (0.23)	0.46 (0.21)	0.56 (0.32)	0.30 (0.21)	0.48 (0.26)
Ac. temp. of 0.2	<i>0.46</i> (0.34)	<i>0.46</i> (0.23)	0.43 (0.22)	0.42 (0.31)	0.27 (0.21)	0.41 (0.26)
Ac. temp. of 0.6	<i>0.50</i> (0.33)	0.47 (0.25)	0.45 (0.23)	0.44 (0.31)	0.29 (0.21)	0.43 (0.27)
Ac. spatial of 0.2	<i>0.49</i> (0.35)	0.46 (0.24)	0.43 (0.23)	0.44 (0.31)	0.33 (0.23)	0.43 (0.27)
Ac. spatial of 0.6	<i>0.47</i> (0.33)	<i>0.47</i> (0.24)	0.45 (0.22)	0.42 (0.31)	0.21 (0.16)	0.40 (0.25)
SNR of 1	0.48 (0.34)	<i>0.50</i> (0.26)	0.47 (0.24)	0.44 (0.33)	0.24 (0.16)	0.43 (0.27)
SNR of 3	<i>0.47</i> (0.34)	0.44 (0.22)	0.41 (0.21)	0.43 (0.28)	0.32 (0.25)	0.41 (0.26)
Pearsons cor.	<i>0.69</i> (0.31)	0.63 (0.10)	0.59 (0.09)	0.58 (0.28)	0.38 (0.19)	0.57 (0.19)
Partial cor.	0.15 (0.09)	<i>0.16</i> (0.11)	<i>0.16</i> (0.12)	<i>0.16</i> (0.14)	0.09 (0.07)	0.14 (0.11)
Circular cor.	<i>0.69</i> (0.27)	0.61 (0.11)	0.57 (0.11)	0.57 (0.26)	0.39 (0.18)	0.57 (0.19)
Coherence	<i>0.38</i> (0.26)	-	-	-	-	0.38 (0.26)
Global average <sup>1</sup>	<b>0.48</b> (0.34)	0.47 (0.24)	0.44 (0.23)	0.43 (0.30)	0.28 (0.21)	0.42 (0.26)

*Note.* In italic are the best performing measures for each level of the manipulated factor. In bold is the best performing measure across all manipulated factors. The cases with a dash correspond to particular combination of factors where for all data sets of that design cell the graph theory measures had no variance and thus the correlation was not defined.

<sup>1</sup> Corresponds to an average across all manipulated factors

In Table 7, the results for the graph theory measures from multiplex networks are presented. The best performing graph theory measure is the degree centrality (mean correlation of .46), no matter the level of the different manipulated factors. The other three measures show a bad performance ( $< .26$ ). The differences in performance between the different levels of the various factors are rather small, even for the transform function, for which way larger differences were observed in the previous tables. It is remarkable that for degree centrality the partial correlation is the best performing transform function.

Table 7

*Average absolute correlation overall and for each level of the manipulated factors (and corresponding standard deviation between parenthesis) for each graph theory measure from multiplex networks.*

	Degree trality	cen- lay coef.	Global lay clust.	over- clust.	Pearsons cor.	Entropy	Overall
16 electrodes	<i>0.45</i> (0.26)	0.23 (0.19)	0.17 (0.12)	0.14 (0.10)	0.25 (0.17)		
32 electrodes	<i>0.47</i> (0.26)	0.27 (0.21)	0.16 (0.12)	0.16 (0.11)	0.27 (0.17)		
1000 time points	<i>0.44</i> (0.27)	0.24 (0.20)	0.16 (0.12)	0.15 (0.11)	0.25 (0.18)		
10000 time points	<i>0.49</i> (0.25)	0.25 (0.21)	0.17 (0.12)	0.15 (0.10)	0.27 (0.17)		
Ac. temp. of 0.2	<i>0.44</i> (0.27)	0.22 (0.21)	0.16 (0.12)	0.14 (0.10)	0.24 (0.17)		
Ac. temp. of 0.6	<i>0.48</i> (0.26)	0.27 (0.19)	0.17 (0.12)	0.16 (0.11)	0.27 (0.17)		
Ac. spatial of 0.2	<i>0.49</i> (0.28)	0.21 (0.17)	0.17 (0.12)	0.15 (0.11)	0.26 (0.17)		
Ac. spatial of 0.6	<i>0.43</i> (0.24)	0.28 (0.23)	0.16 (0.12)	0.15 (0.10)	0.26 (0.17)		
SNR of 1	<i>0.48</i> (0.24)	0.24 (0.21)	0.17 (0.14)	0.14 (0.10)	0.26 (0.17)		
SNR of 3	<i>0.45</i> (0.28)	0.26 (0.20)	0.16 (0.10)	0.16 (0.11)	0.26 (0.17)		
Pearsons cor.	<i>0.48</i> (0.26)	0.33 (0.19)	0.17 (0.11)	0.18 (0.13)	0.29 (0.17)		
Partial cor.	<i>0.53</i> (0.24)	0.10 (0.10)	0.19 (0.12)	0.14 (0.09)	0.24 (0.14)		
Circular cor.	<i>0.38</i> (0.29)	0.33 (0.22)	0.15 (0.13)	0.13 (0.09)	0.25 (0.18)		
Coherence	<i>0.46</i> (0.25)	0.23 (0.18)	0.15 (0.12)	0.16 (0.11)	0.25 (0.17)		
Global average <sup>1</sup>	<b>0.46</b> (0.26)	0.25 (0.20)	0.16 (0.12)	0.15 (0.10)	0.26 (0.17)		

*Note.* In italic are the best performing measures for each level of the manipulated factor. In bold is the best performing measure across all manipulated factors.

<sup>1</sup> Corresponds to an average across all manipulated factors

From Table 8, which presents the results for temporal networks, it appears that the density is the only measure with a somewhat satisfactory performance level (mean correlation of .32); the other measures perform really bad ( $< .08$ ). The density is the best method, no matter the level of the different manipulated factors. As observed in previous tables, performance

is best for less electrodes, more time points and when using Pearson's and the circular correlation.

Table 8

*Average absolute correlation overall and for each level of the manipulated factors (and corresponding standard deviation between parenthesis) for each graph theory measure from temporal networks.*

	Density	Avg. de- gree	Clos. centr.	Betw. centr.	Avg. compo- nent	Avg. edge formation	Overall
16 electrodes	<i>0.36</i> (0.24)	0.08 (0.08)	0.10 (0.05)	0.07 (0.05)	0.08 (0.06)	0.03 (0.02)	0.12 (0.08)
32 electrodes	<i>0.28</i> (0.20)	0.05 (0.04)	0.05 (0.04)	0.04 (0.03)	0.04 (0.04)	0.02 (0.02)	0.08 (0.06)
1000 time points	<i>0.24</i> (0.17)	0.08 (0.08)	0.08 (0.05)	0.06 (0.05)	0.07 (0.05)	0.03 (0.02)	0.09 (0.07)
10000 time points	<i>0.40</i> (0.24)	0.05 (0.03)	0.06 (0.05)	0.05 (0.05)	0.06 (0.05)	0.02 (0.02)	0.11 (0.07)
Ac. temp. of 0.2	<i>0.33</i> (0.21)	0.07 (0.06)	0.06 (0.05)	0.05 (0.05)	0.06 (0.05)	0.03 (0.02)	0.10 (0.07)
Ac. temp. of 0.6	<i>0.31</i> (0.23)	0.06 (0.06)	0.08 (0.06)	0.06 (0.05)	0.06 (0.06)	0.02 (0.02)	0.10 (0.08)
Ac. spatial of 0.2	<i>0.33</i> (0.22)	0.07 (0.06)	0.07 (0.06)	0.06 (0.05)	0.06 (0.06)	0.03 (0.02)	0.10 (0.08)
Ac. spatial of 0.6	<i>0.31</i> (0.23)	0.06 (0.06)	0.07 (0.05)	0.06 (0.05)	0.06 (0.05)	0.02 (0.02)	0.10 (0.08)
SNR of 1	<i>0.32</i> (0.23)	0.07 (0.08)	0.06 (0.05)	0.05 (0.04)	0.05 (0.05)	0.02 (0.02)	0.10 (0.08)
SNR of 3	<i>0.33</i> (0.22)	0.06 (0.04)	0.08 (0.06)	0.06 (0.06)	0.07 (0.06)	0.03 (0.02)	0.11 (0.08)
Pearsons cor.	<i>0.43</i> (0.22)	0.08 (0.05)	0.09 (0.05)	0.08 (0.05)	0.08 (0.05)	0.03 (0.02)	0.13 (0.07)
Partial cor.	<i>0.15</i> (0.10)	0.03 (0.03)	0.03 (0.02)	0.03 (0.02)	0.03 (0.03)	0.03 (0.02)	0.05 (0.04)
Circular cor.	<i>0.44</i> (0.21)	0.09 (0.06)	0.10 (0.06)	0.08 (0.05)	0.09 (0.06)	0.02 (0.02)	0.14 (0.08)
Coherence	<i>0.26</i> (0.20)	0.06 (0.08)	0.04 (0.04)	0.04 (0.04)	0.04 (0.03)	0.03 (0.02)	0.08 (0.07)
Global average <sup>1</sup>	<b>0.32</b> (0.22)	0.07 (0.06)	0.07 (0.05)	0.06 (0.05)	0.06 (0.05)	0.03 (0.02)	0.10 (0.07)

*Note.* In italic are the best performing measures for each level of the manipulated factor. In bold is the best performing measure across all manipulated factors.

<sup>1</sup> Corresponds to an average across all manipulated factors

The results with the signed correlation are presented in Appendix B. The largest differences with the absolute correlation results are the following: (1) the partial correlation is always close

to 0 no matter which graph theory measures is considered, (2) the correlation for global clustering coefficient from unweighted network is close to 0 and (3) the correlation for degree centrality from multiplex network is close to 0. This close to zero (raw) correlation implies that positive and negative correlation values are averaged out. It appears that in these instances the sign of the correlation is rather random, which implies that performance is bad.

## 4.2 Influence of design factors

To study the influence of the design factors, we first performed a mixed ANOVA using all manipulated factors (and not estimating the highest order interaction, see Section 3.6). From this analysis, of which the results are presented in Table 9 for the main effects - see Appendix C for the full table - it appears that performance does not depend much on the amount of temporal and spatial autocorrelation and the signal to noise ratio (SNR). These factors are also not involved in any substantial interaction effect. Therefore, we decided to remove the two autocorrelation factors from the design; we kept the SNR factor as we were especially interested in its effect.

Table 9

*Main effects of the mixed model ANOVA results (using all manipulated factors).*

	Sum Sq	num Df	Error SS	den Df	F value	<sup>1</sup>
n_electrodes	11.07	1.00	0.01	1.00	1238.15	*
n_time_points	50.75	1.00	0.01	1.00	5677.10	**
signal_to_noise	0.25	1.00	0.01	1.00	28.23	
autocor_temporel	0.32	1.00	0.01	1.00	35.39	
autocor_spatial	0.31	1.00	0.01	1.00	34.82	
measure	218.99	21.00	1.63	21.00	134.34	.
transform_function	99.69	3.00	0.20	3.00	497.76	*

<sup>1</sup> The presented p-values are adjusted with the Greenhouse-Geisser correction  $\hat{\epsilon}$  for lack of sphericity, which is the case for all effects with more than one degree of freedom in the numerator.

.  $p < 0.1$ . \*  $p < 0.05$ . \*\*  $p < 0.01$ .

Next, we ran a new mixed ANOVA without the two autocorrelation factors. Because now we have multiple observations per design cell, we were able to fit a full-factorial (mixed) ANOVA in order to study all main and interaction effects between manipulated factors. As this is a simulation study (with large sample sizes), most effects were significant at the .05 level. To simplify results, we only focused on the effects with a substantial effect size (for the full ANOVA results, see Appendix D). In order to calculate the effect sizes, we used the generalized eta squared  $\eta_G^2$ ,

which is recommended for mixed model ANOVA by Bakeman (2005). In the following, only effects with an effect size larger than .26 will be discussed, which are presented in Table 10.

Table 10

*Mixed model ANOVA results (excluding the temporal and spatial autocorrelation factor), only showing main and interaction effects with an effect size (estimated by generalized eta squared) above .26.*

	Sum Sq	num Df	Error SS	den Df	F value	<sup>1</sup> $\eta_G^2$
n_electrodes	11.07	1.00	3.40	24.00	78.11 ***	0.50
n_timepoints	50.75	1.00	3.40	24.00	358.14 ***	0.82
measure	218.99	21.00	16.27	504.00	323.08 ***	0.80
n_timepoints:measure	43.33	21.00	16.27	504.00	63.92 ***	0.45
transform_function	99.69	3.00	4.02	72.00	595.14 ***	0.88
n_timepoints $\times$ transform_function	16.02	3.00	4.02	72.00	95.65 ***	0.55
measure $\times$ transform_function	115.73	63.00	55.64	1512.00	49.92 ***	0.39

<sup>1</sup> The presented p-values are adjusted with the Greenhouse-Geisser correction  $\hat{\epsilon}$  for lack of sphericity, which is the case for all effects with more than one degree of freedom in the numerator.

\*\*\*  $p < 0.001$ .

First, a large interaction effect was observed between the number of time points and the transform function ( $F = 95.65, p_{GG} < 0.001, \eta_G^2 = 0.55$ ). We can see in Figure 10 that the best performance results are obtained for both the Pearson's correlation and circular correlation and the worst for the partial correlation. In general, performance became a bit better when the number of time points increased. Regarding the interaction between transform function and number of times points, a larger number of timepoints provided stronger correlations between the true interbrain value and the different graph theory measures for all transform functions except for the partial correlation for which the reverse was true. The positive performance effect of the number of time points was larger for the Pearson's and the circular transform function than for the coherence transform function.

Next, a large interaction effect was also observed between the transform function and the graph theory measures ( $F = 49.92, p_{GG} < 0.001, \eta_G^2 = 0.39$ ). We can see in Figure 11 that, in general, the Pearson's correlation and the circular correlation performed better in terms of capturing synchrony than the coherence and the partial correlation; the coherence function slightly outperforms the partial correlation transform function. This performance pattern is clearly observed for the graph theory measures from the weighted and unweighted networks as well as for the global overlay clustering coefficient (multiplex network), the density (temporal network) and

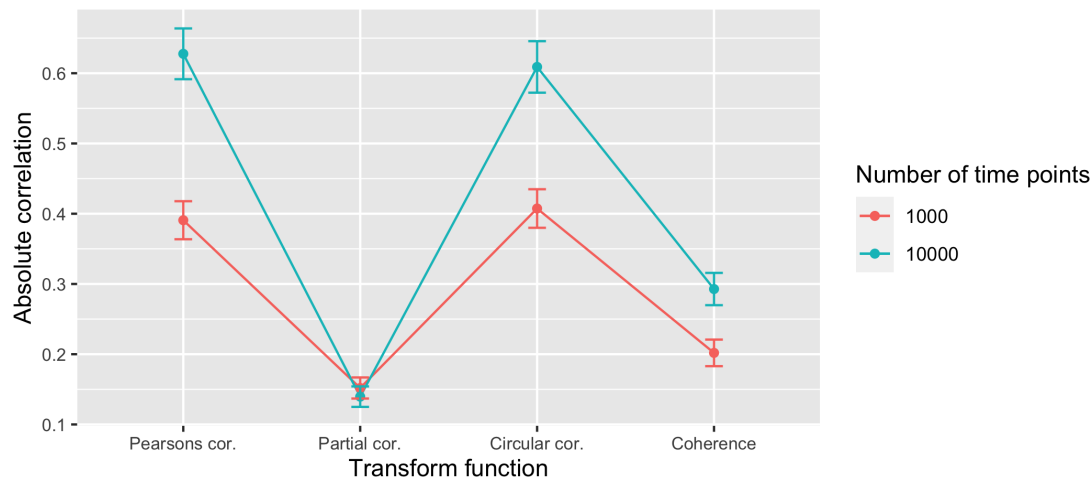


*Figure 10.* Interaction between the number of timepoints and the transform function used regarding the absolute correlation between the interbrain value and the different graph theory measures. The averaged absolute correlation is presented with its corresponding confidence interval.

the one measure from the bipartite network (i.e., the averaged strength). For the other network measures, the transform functions perform at a very similar level.

Thirdly, a large interaction effect was observed between the number of time points and the graph theory measures ( $F = 63.92, p_{GG} < 0.001, n_G^2 = 0.45$ ). We can see in Figure 12 that for the graph theory measures from weighted, unweighted and bipartite networks (except for the global clustering coefficient applied to unweighted networks), a larger number of time points provided a stronger correlation between the true interbrain value and the different graph theory measures than a smaller number of time points. This worked the other way around for the graph theory measures from temporal networks. For graph theory measures from multiplex network, the number of time points did not result in sizeable performance differences.

Lastly, a large main effect was observed for the number of electrodes used ( $F = 78.11, p < 0.001, n_G^2 = 0.50$ ). Having less electrodes resulted in larger correlations between the simulation interbrain value and the different graph theory measures than having a larger number of electrodes. The average absolute correlation for 16 electrode is 0.389 with 95% confidence interval (0.372, 0.405) and for 32 electrodes, this value is 0.316 with 95% confidence interval (0.301, 0.331).

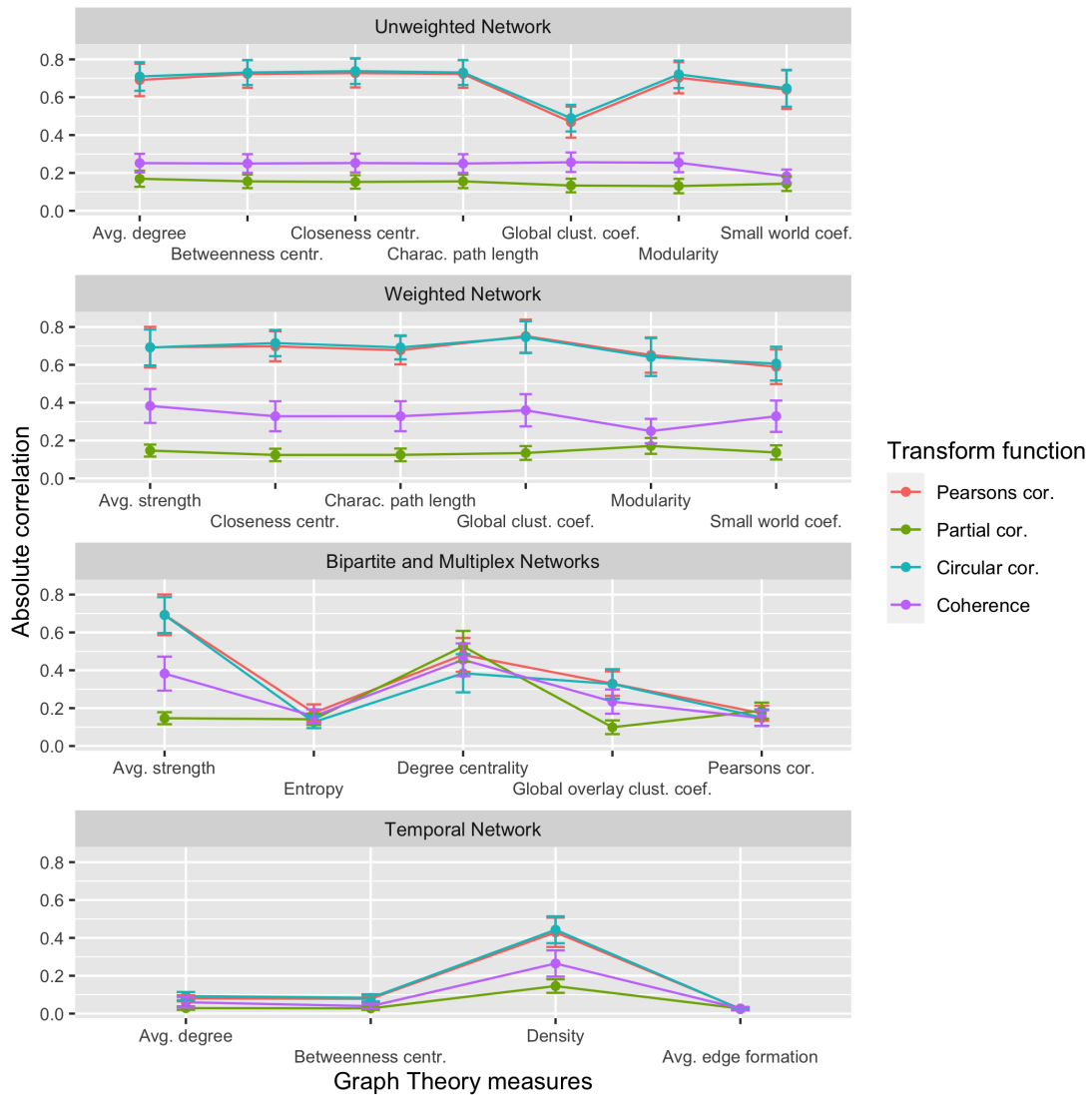


*Figure 11.* Interaction between the transform functions and the graph theory measures for the the absolute correlation between the interbrain value and the different graph theory measures. The averaged absolute correlation is presented with its corresponding confidence interval. The graph theory measures are presented separately per type of network (topologies) they are applied to. Bipartite and multiplex network measures are presented together as only the average strength is a bipartite network measure.

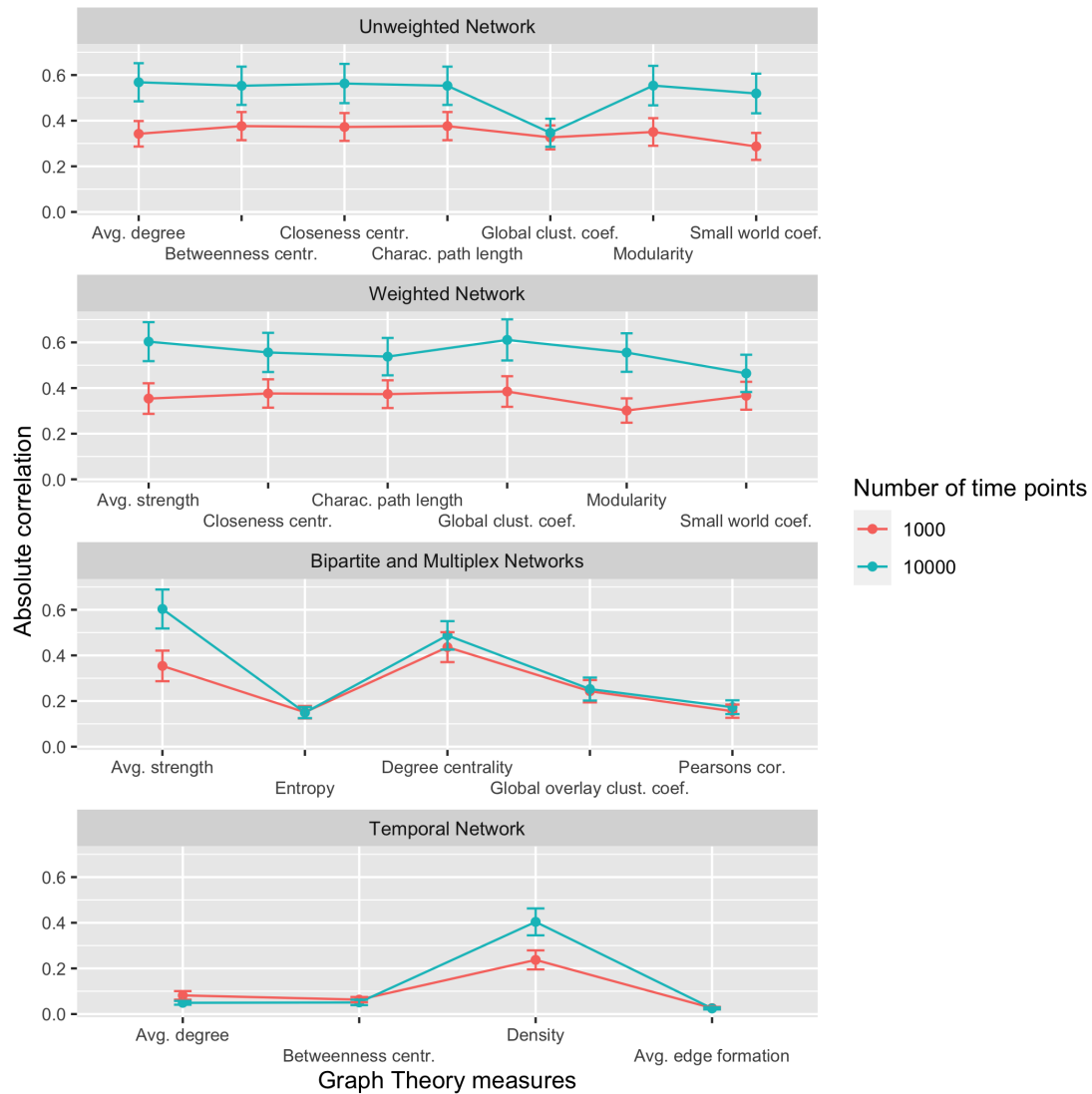


Figure 12. Interaction between the number of timepoints and the graph theory measures regarding the absolute correlation between the interbrain value and the different graph theory measures. The averaged absolute correlation is presented with its corresponding confidence interval. The graph theory measures are presented in separate panels, grouping measures obtained from the same type of network (topologies) they are applied to. Bipartite and multiplex networks measures are presented together as only the average strength is a bipartite network measure.



# Discussion

The aim of this thesis was to fill in the gap in the literature regarding the use of complex network analysis methods as a tool to detect interpersonal synchrony in EEG data. To this end, a simulation study was conducted to allow a systematic comparison between several graph theory measures that are derived from different types of networks (topologies) regarding their capability to capture synchrony. It was also studied how the performance of the graph theory measures depends on varying input parameter characteristics of EEG data and different transform functions used for the transformation of the data to accommodate a complex network analysis. In the next sections, the main results of this simulation will be discussed, along with the limitations of the simulation study, before presenting some concluding remarks.

## 5.1 Main results

From the results of our simulation study, we gather that a lot of graph theory measures were able to accurately detect changes in interpersonal synchrony, with the best method, the global clustering coefficient for weighted network, resulting in a .50 correlation on average between the given graph theory measure and the actual interpersonal synchrony value. Multiple measures performed on a similar level for unweighted networks: the average degree, closeness centrality, betweenness centrality, characteristic path length and modularity. For the bipartite networks, the average strength and connectance performed best. All measures previously mentioned performed at very similar levels. For temporal networks, the density performed best, although substantially lower than the best performing method(s) for other types of networks. For the multiplex networks, the degree centrality performed best (at the level of the best methods in the study), but this result must be taken with a grain of salt as the average signed correlation was close to 0. This means that the degree centrality was in equal amounts positively and negatively correlated to the interbrain value, which seems to suggest that the sign of the correlation is a bit

random.

Our results also corroborate earlier findings concerning the links between synchrony and some of the weighted graph theory measures (Müller and Lindenberger, 2014; Müller et al., 2013; Sängler et al., 2012). In their different activities requiring highly coordinated interpersonal behaviour (such as guitar duet, guitar improv and kissing) a higher synchrony of the oscillatory activity of the brain was observed as well as increased strength and small world coefficient, as well as shorter characteristic path length, which is also what was observed here (see Table 12 in Appendix B).

Another key finding of this simulation study is the importance of some of the manipulated factors of the study design. Among the most important factors are the length of the EEG recordings (i.e., the number of time points) and the function used for the transformation of the data to a network. As such, for all functions except for the partial correlation, a lengthier EEG recording is beneficial to the measure of interpersonal synchrony. Actually, the use of partial correlation to transform the data made it barely possible to detect interpersonal synchrony altogether, which makes sense considering its disregard of the spatial correlation between electrodes - hence its absence in the scientific literature concerning synchrony. Pearson's correlation and circular correlation were the best transform functions to use when looking for synchrony in network data, whereas coherence performed substantially worse. This is different than what was predicted, as we expected linear measures (i.e., Pearson's correlation, partial correlation, and coherence) to yield more similar results (Dauwels et al., 2010). It was, however, the circular correlation that performed at the same level as the Pearson's correlation. Note that all the previously mentioned graph theory measures (except for the global clustering coefficient from the unweighted networks) performed better with lengthier EEG recordings and when the data was transformed using the Pearson's or the circular correlation. Surprisingly, having fewer electrodes made it easier to detect synchrony. This may be linked to the fact that the number of nodes is part of the calculation of almost all graph theory measures. A higher number of nodes means more variance in graph theory measures, hence making it harder to detect the correlation between the interbrain value and those measures. Before going further, it is of particular interest to us to mention that the signal to noise ratio did not have even a small main effect or interaction effect with any of the other factors. This implies that the use of graph theory measures to detect interpersonal synchrony seems to be resistant to the presence of noise in the data.

## 5.2 Limitations and future research

However, our simulation is not without limitations. The simulation study was developed with flexibility in mind, as a lot of parameters could be manipulated, and was not especially tuned to generate data with typical EEG behaviour. Of course, we had to limit in our study the number of values for each parameter as this simulation was already computationally intensive. Moreover, other parameter sets could (and should) be tested in further studies, like the values for the number and length of the time windows for the temporal networks, and the threshold values for unweighted and temporal networks. The influence of these parameters on the performance results was not studied in this thesis as these values were fixed to a particular number. We also fixed the size of the difference between the interbrain and intrabrain value.

Concerning graph theory measures, most of those coming from bipartite networks had to be discarded as they presented no variance for sets of parameters, so the use of a threshold may be necessary here to get more out of them. Bipartite networks have, to our knowledge, not been used for any brain data, and as such a lot of graph theory measures from this topology could not be applied as they are irrelevant. Also, both temporal and multiplex networks have limited literature on how to incorporate weights in their networks, which would most certainly make their graph theory measures more relevant here. Moreover, the graph theory measures coming from multiplex networks barely, if ever, consider interlayer links. For this thesis, this means that we are not taking advantage of the between participants' correlation values to determine synchrony. Finally, due to the comparison being made across multiple types of network topologies, the temporal dimension of temporal networks was not investigated here, but would definitely be appropriate to study in future research like the size of the time window, if they overlap or not, etc.

Concerning our analysis of the results, the choice was made to study the performance of different graph theory measures to detect differences in interpersonal synchrony using the correlation between mentioned graph theory measures and the generated true interbrain value. This was a valid approach to take but other approaches could have been taken. In fact, the decision to use correlation made us lose our replicates for the remainder of the analysis, as we used them to calculate the (absolute) correlation values.

Future research could focus on the directed counterpart of the tested networks and take advantage of the added level of complexity it entails. Moreover, for the analysis of our results, each network measure was reduced to a single value, their mean, whenever it was needed (e.g., the

degree or the betweenness centrality). But for these measures, we could consider their distribution rather than their average. Lastly, standardized versions (with regard to the number of nodes in the network) of some of the graph theory network exists, and could also be investigated.

### **5.3 Concluding remarks**

In this thesis, we studied the appropriateness of several graph theory measure to capture change in interpersonal synchrony. Some measures clearly outperformed others, with the best measure being the global clustering coefficient from the weighted network. In general, measures from weighted and unweighted networks performed well, especially in combination with the Pearson's correlation and the circular correlation transform function. Measures from temporal and multiplex network performed poorly. In general, the graph theory measures performed better with longer recordings and less electrodes. All in all, complex network analysis and the associated graph theory measures are most definitely useful tools for future research into interpersonal synchrony.

# Bibliography

- Adah, T., & Ortega, A. (2018). Applications of Graph Theory [Scanning the Issue]. *Proceedings of the IEEE*, 106(5), 784–786. doi:10.1109/JPROC.2018.2820300
- Agostinelli, C., & Lund, U. (2017). *R package circular: Circular Statistics (version 0.4-93)*. Manual. CA: Department of Environmental Sciences, Informatics and Statistics, Ca' Foscari University, Venice, Italy. UL: Department of Statistics, California Polytechnic State University, San Luis Obispo, California, USA. Retrieved from <https://r-forge.r-project.org/projects/circular/>
- Almeida-Neto, M., & Ulrich, W. (2011). A straightforward computational approach for measuring nestedness using quantitative matrices. *Environmental Modelling & Software*, 26(2), 173–178. doi:10.1016/j.envsoft.2010.08.003
- Anastasiadou, M. N., Christodoulakis, M., Papathanasiou, E. S., Papacostas, S. S., Hadjipapas, A., & Mitsis, G. D. (2019). Graph Theoretical Characteristics of EEG-Based Functional Brain Networks in Patients With Epilepsy: The Effect of Reference Choice and Volume Conduction. *Front. Neurosci.* 13. doi:10.3389/fnins.2019.00221
- Bakeman, R. (2005). Recommended effect size statistics for repeated measures designs. *Behavior Research Methods*, 37(3), 379–384. doi:10.3758/BF03192707
- Battiston, F., Nicosia, V., & Latora, V. (2014). Structural measures for multiplex networks. *Phys. Rev. E*, 89(3), 032804. doi:10.1103/PhysRevE.89.032804. arXiv: 1308.3182
- Bender-deMoll, S., & Morris, M. (2021). *Tsna: Tools for Temporal Social Network Analysis*. Manual. Retrieved from <https://CRAN.R-project.org/package=tsna>
- Brandes, U. (2001). A faster algorithm for betweenness centrality. *The Journal of Mathematical Sociology*, 25(2), 163–177. doi:10.1080/0022250X.2001.9990249
- Buldú, J. M., & Porter, M. A. (2018). Frequency-based brain networks: From a multiplex framework to a full multilayer description. *Netw Neurosci*, 2(4), 418–441. doi:10.1162/netn\_a.00033. pmid: 30294706

- Bullmore, E., & Sporns, O. (2009). Complex brain networks: Graph theoretical analysis of structural and functional systems. *Nature Reviews Neuroscience*, *10*(3), 186–198. doi:10.1038/nrn2575
- Burgess, A. P. (2013). On the interpretation of synchronization in EEG hyperscanning studies: A cautionary note. *Front Hum Neurosci*, *7*. doi:10.3389/fnhum.2013.00881. pmid: 24399948
- Chai, M. T., Amin, H. U., Izhar, L. I., Saad, M. N. M., Abdul Rahman, M., Malik, A. S., & Tang, T. B. (2019). Exploring EEG Effective Connectivity Network in Estimating Influence of Color on Emotion and Memory. *Front Neuroinform*, *13*. doi:10.3389/fninf.2019.00066. pmid: 31649522
- Christensen, A. P. (2018). NetworkToolbox: Methods and Measures for Brain, Cognitive, and Psychometric Network Analysis in R. *10*, 18.
- Cirelli, L. K., Wan, S. J., & Trainor, L. J. (2014). Fourteen-month-old infants use interpersonal synchrony as a cue to direct helpfulness. *Philos Trans R Soc Lond B Biol Sci*, *369*(1658). doi:10.1098/rstb.2013.0400. pmid: 25385778
- Clauset, A., Newman, M. E. J., & Moore, C. (2004). Finding community structure in very large networks. *Phys. Rev. E*, *70*(6), 066111. doi:10.1103/PhysRevE.70.066111. arXiv: cond-mat/0408187
- Czeszumski, A., Eustergerling, S., Lang, A., Menrath, D., Gerstenberger, M., Schubert, S., ... König, P. (2020). Hyperscanning: A Valid Method to Study Neural Inter-brain Underpinnings of Social Interaction. *Front. Hum. Neurosci.* *14*, 39. doi:10.3389/fnhum.2020.00039
- Dauwels, J., Vialatte, F., & Cichocki, A. (2010). A Comparative Study of Synchrony Measures for the Early Detection of Alzheimer's Disease Based on EEG, 10.
- De Domenico, M., Solé-Ribalta, A., Cozzo, E., Kivela, M., Moreno, Y., Porter, M. A., ... Arenas, A. (2013). Mathematical Formulation of Multilayer Networks. *Phys. Rev. X*, *3*(4), 041022. doi:10.1103/PhysRevX.3.041022
- Degani, E. (2017). *Mplex: Mplex*. Manual. Retrieved from <https://github.com/Achab94/mplex>
- Dormann, C. F., Frund, J., Bluthgen, N., & Gruber, B. (2009). Indices, Graphs and Null Models: Analyzing Bipartite Ecological Networks. *TOECOLJ*, *2*(1), 7–24. doi:10.2174/1874213000902010007
- Dunne, J. A., Williams, R. J., & Martinez, N. D. (2002). Network structure and biodiversity loss in food webs: Robustness increases with connectance. *Ecol Letters*, *5*(4), 558–567. doi:10.1046/j.1461-0248.2002.00354.x

- Epskamp, S., Cramer, A. O. J., Waldorp, L. J., Schmittmann, V. D., & Borsboom, D. (2012). Qgraph: Network Visualizations of Relationships in Psychometric Data. *Journal of Statistical Software*, *48*, 1–18. doi:10.18637/jss.v048.i04
- Feld, S. L. (1991). Why Your Friends Have More Friends Than You Do. *American Journal of Sociology*, *96*(6), 1464–1477. doi:10.1086/229693
- Fox, J., & Weisberg, S. (2019). *An R Companion to Applied Regression*. Thousand Oaks, CA: Sage. Retrieved February 9, 2022, from <https://socialsciences.mcmaster.ca/jfox/Books/Companion/>
- Geisser, S., & Greenhouse, S. W. (1958). An Extension of Box's Results on the Use of the  $F$  Distribution in Multivariate Analysis. *The Annals of Mathematical Statistics*, *29*(3), 885–891. doi:10.1214/aoms/1177706545
- Genz, A., Bretz, F., Miwa, T., Leisch, F., Scheipl, F., & Hothorn, T. (2021). *Mvtnorm: Multivariate Normal and t Distributions*. Manual. Retrieved from <https://CRAN.R-project.org/package=mvtnorm>
- Ghahari, S., Salehi, F., Farahani, N., Coben, R., & Motie Nasrabadi, A. (2020). Representing Temporal Network based on dDTF of EEG signals in Children with Autism and Healthy Children. *Biomedical Signal Processing and Control*, *62*, 102139. doi:10.1016/j.bspc.2020.102139
- Hastie, T., Tibshirani, R., & Friedman, J. (2009). *The Elements of Statistical Learning: Data Mining, Inference, and Prediction, Second Edition* (2nd ed.). Springer Series in Statistics. doi:10.1007/978-0-387-84858-7
- Hoehl, S., Fairhurst, M., & Schirmer, A. (2021). Interactional synchrony: Signals, mechanisms and benefits. *Soc Cogn Affect Neurosci*, *16*(1-2), 5–18. doi:10.1093/scan/nsaa024
- Humphries, M. D., & Gurney, K. (2008). Network 'Small-World-Ness': A Quantitative Method for Determining Canonical Network Equivalence. *PLOS ONE*, *3*(4), e0002051. doi:10.1371/journal.pone.0002051
- Ikeda, S., Nozawa, T., Yokoyama, R., Miyazaki, A., Sasaki, Y., Sakaki, K., & Kawashima, R. (2017). Steady Beat Sound Facilitates both Coordinated Group Walking and Inter-Subject Neural Synchrony. *Front. Hum. Neurosci.* *11*. doi:10.3389/fnhum.2017.00147
- Joo, R., Etienne, M.-P., Bez, N., & Mahévas, S. (2018). Metrics for describing dyadic movement: A review. *Mov Ecol*, *6*(1), 26. doi:10.1186/s40462-018-0144-2

- Kim, S. (2015). Ppcor: An R Package for a Fast Calculation to Semi-partial Correlation Coefficients. *Commun Stat Appl Methods*, 22(6), 665–674. doi:10.5351/CSAM.2015.22.6.665. pmid: 26688802
- Konvalinka, I., Xygalatas, D., Bulbulia, J., Schjødt, U., Jegindø, E.-M., Wallot, S., . . . Roepstorff, A. (2011). Synchronized arousal between performers and related spectators in a fire-walking ritual. *PNAS*, 108(20), 8514–8519. doi:10.1073/pnas.1016955108. pmid: 21536887
- Koole, S. L., & Tschacher, W. (2016). Synchrony in Psychotherapy: A Review and an Integrative Framework for the Therapeutic Alliance. *Front. Psychol.* 7. doi:10.3389/fpsyg.2016.00862
- Kwong, K. K., Belliveau, J. W., Chesler, D. A., Goldberg, I. E., Weisskoff, R. M., Poncelet, B. P., . . . Turner, R. (1992). Dynamic magnetic resonance imaging of human brain activity during primary sensory stimulation. *Proc Natl Acad Sci U S A*, 89(12), 5675–5679. pmid: 1608978. Retrieved October 27, 2021, from <https://www.ncbi.nlm.nih.gov/pmc/articles/PMC49355/>
- Liu, S., Gates, K. M., & Bandon, A. Y. (2018). Directly assessing interpersonal RSA influences in the frequency domain: An illustration with generalized partial directed coherence. *Psychophysiology*, 55(6), e13054. doi:10.1111/psyp.13054
- Mashaghi, A. R., Ramezanpour, A., & Karimipour, V. (2004). Investigation of a protein complex network. *Eur. Phys. J. B*, 41(1), 113–121. doi:10.1140/epjb/e2004-00301-0
- Müller, V., & Lindenberger, U. (2014). Hyper-Brain Networks Support Romantic Kissing in Humans. *PLOS ONE*, 9(11), e112080. doi:10.1371/journal.pone.0112080
- Müller, V., Sängler, J., & Lindenberger, U. (2013). Intra- and Inter-Brain Synchronization during Musical Improvisation on the Guitar. *PLOS ONE*, 8(9), e73852. doi:10.1371/journal.pone.0073852
- Naro, A., Maggio, M. G., Leo, A., & Calabrò, R. S. (2021). Multiplex and Multilayer Network EEG Analyses: A Novel Strategy in the Differential Diagnosis of Patients with Chronic Disorders of Consciousness. *Int J Neural Syst*, 31(2), 2050052. doi:10.1142/S0129065720500525. pmid: 33034532
- Newman, M. E. J. (2001). Scientific collaboration networks. II. Shortest paths, weighted networks, and centrality. *Phys. Rev. E*, 64(1), 016132. doi:10.1103/PhysRevE.64.016132
- Nicosia, V., & Latora, V. (2015). Measuring and modeling correlations in multiplex networks. *Physical Review E*, 92, 032805. doi:10.1103/PhysRevE.92.032805

- Nowak, A., Vallacher, R. R., Zochowski, M., & Rychwalska, A. (2017). Functional Synchronization: The Emergence of Coordinated Activity in Human Systems. *Front. Psychol.* 8. doi:10.3389/fpsyg.2017.00945
- Onnela, J.-P., Saramäki, J., Kertész, J., & Kaski, K. (2005). Intensity and coherence of motifs in weighted complex networks. *Phys. Rev. E*, 71(6), 065103. doi:10.1103/PhysRevE.71.065103
- Opsahl, T., Agneessens, F., & Skvoretz, J. (2010). Node centrality in weighted networks: Generalizing degree and shortest paths. *Social Networks*, 32(3), 245–251. doi:10.1016/j.socnet.2010.03.006
- Pilowsky, J. (2020). *Colorednoise: Simulate Temporally Autocorrelated Populations*. Manual. Retrieved from <https://CRAN.R-project.org/package=colorednoise>
- Piperski, A. (2014). An application of graph theory to linguistic complexity. *Yearbook of the Poznan Linguistic Meeting*, 1(1), 89–102. doi:10.1515/yplm-2015-0005
- R Core Team. (2020). R : A language and environment for statistical computing. R Foundation for Statistical Computing. Vienna, Austria. Retrieved from <https://www.R-project.org/>
- Sänger, J., Müller, V., & Lindenberger, U. (2012). Intra- and interbrain synchronization and network properties when playing guitar in duets. *Front. Hum. Neurosci.* 6. doi:10.3389/fnhum.2012.00312
- Seraj, E. (2018). Cerebral Synchrony Assessment Tutorial: A General Review on Cerebral Signals' Synchronization Estimation Concepts and Methods. arXiv: 1612.04295 [q-bio]. Retrieved January 20, 2021, from <http://arxiv.org/abs/1612.04295>
- Sueur, J., Aubin, T., & Simonis, C. (2008). Seewave, a free modular tool for sound analysis and synthesis. *Bioacoustics*, 18, 213–226. doi:10.1080/09524622.2008.9753600
- Szűcs, D., & Csépe, V. (2004). Access to numerical information is dependent on the modality of stimulus presentation in mental addition: A combined ERP and behavioral study. *Cognitive Brain Research*, 19(1), 10–27. doi:10.1016/j.cogbrainres.2003.11.002
- Thompson, W. H., Brantefors, P., & Fransson, P. (2017). From static to temporal network theory: Applications to functional brain connectivity. *Network Neuroscience*, 1(2), 69–99. doi:10.1162/NETN\_a.00011
- Travers, J., & Milgram, S. (1969). An Experimental Study of the Small World Problem. *Sociometry*, 32(4), 425. doi:10.2307/2786545. JSTOR: 2786545
- van Wijk, B. C. M., Stam, C. J., & Daffertshofer, A. (2010). Comparing Brain Networks of Different Size and Connectivity Density Using Graph Theory. *PLOS ONE*, 5(10), e13701. doi:10.1371/journal.pone.0013701

- 
- Watts, D. J., & Strogatz, S. H. (1998). Collective dynamics of ‘small-world’ networks. *Nature*, *393*(6684), 440–442. doi:10.1038/30918
- Wiltermuth, S. S., & Heath, C. (2009). Synchrony and Cooperation. *Psychol Sci*, *20*(1), 1–5. doi:10.1111/j.1467-9280.2008.02253.x
- Yang, H., Ang, K. K., Wang, C., Phua, K. S., & Guan, C. (2016). Chapter 7 - Neural and cortical analysis of swallowing and detection of motor imagery of swallow for dysphagia rehabilitation—A review. In D. Coyle (Ed.), *Progress in Brain Research* (Vol. 228, pp. 185–219). Brain-Computer Interfaces: Lab Experiments to Real-World Applications. doi:10.1016/bs.pbr.2016.03.014
- Yun, K., Watanabe, K., & Shimojo, S. (2012). Interpersonal body and neural synchronization as a marker of implicit social interaction. *Sci Rep*, *2*(1), 959. doi:10.1038/srep00959
- Zhang, J., Kucyi, A., Raya, J., Nielsen, A. N., Nomi, J. S., Damoiseaux, J. S., . . . Whitfield-Gabrieli, S. (2021). What have we really learned from functional connectivity in clinical populations? *NeuroImage*, *242*, 118466. doi:10.1016/j.neuroimage.2021.118466

# Appendices

## A Correlation between graph theory measures

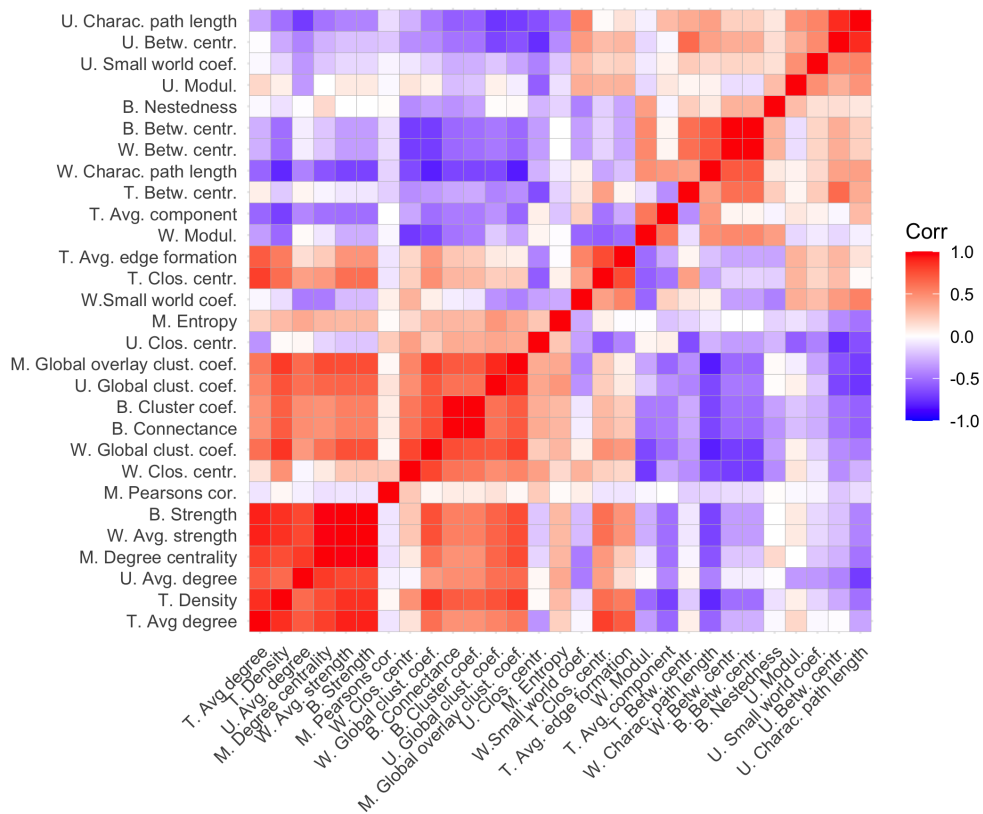


Figure 13. Heatmap of correlations between graph theory measures. The correlation matrix is ordered using a hierarchical clustering function. The first letter of each label corresponds to the network topology of each graph theory measure (i.e., U for unweighted network, W for weighted network, B for bipartite network, M for multiplex network and T for temporal network).

## B Summary tables with signed correlation

Table 11

*Average correlation overall and for each level of the manipulated factors (and corresponding standard deviation between parenthesis) for each graph theory measure from unweighted networks.*

	Clos. centr.	Avg. degree	Global clust. coef.	Small world coef.	Betw. centr.	Charac. path length	Modul.	Overall
16 electrodes	0.44 (0.41)	0.43 (0.42)	-0.03 (0.49)	-0.37 (0.43)	-0.44 (0.41)	-0.44 (0.41)	-0.43 (0.41)	-0.12 (0.43)
32 electrodes	0.35 (0.39)	0.33 (0.38)	-0.17 (0.27)	-0.27 (0.39)	-0.35 (0.39)	-0.35 (0.39)	-0.34 (0.38)	-0.11 (0.37)
1000 time points	0.29 (0.34)	0.27 (0.32)	-0.22 (0.32)	-0.20 (0.32)	-0.30 (0.34)	-0.30 (0.34)	-0.28 (0.33)	-0.11 (0.33)
10000 time points	0.50 (0.44)	0.49 (0.45)	0.01 (0.43)	-0.44 (0.45)	-0.49 (0.43)	-0.49 (0.43)	-0.50 (0.43)	-0.13 (0.44)
Ac. temp. of 0.2	0.39 (0.40)	0.38 (0.39)	-0.12 (0.38)	-0.33 (0.39)	-0.39 (0.40)	-0.39 (0.40)	-0.38 (0.39)	-0.12 (0.39)
Ac. temp. of 0.6	0.40 (0.41)	0.37 (0.42)	-0.09 (0.41)	-0.30 (0.43)	-0.39 (0.41)	-0.39 (0.41)	-0.39 (0.40)	-0.11 (0.41)
Ac. spatial of 0.2	0.41 (0.39)	0.38 (0.40)	-0.12 (0.38)	-0.31 (0.42)	-0.40 (0.39)	-0.40 (0.39)	-0.40 (0.39)	-0.12 (0.39)
Ac. spatial of 0.6	0.39 (0.42)	0.37 (0.41)	-0.09 (0.41)	-0.33 (0.40)	-0.38 (0.42)	-0.38 (0.42)	-0.38 (0.40)	-0.11 (0.41)
SNR of 1	0.39 (0.40)	0.38 (0.40)	-0.16 (0.42)	-0.31 (0.41)	-0.39 (0.40)	-0.39 (0.40)	-0.39 (0.39)	-0.12 (0.40)
SNR of 3	0.40 (0.41)	0.38 (0.41)	-0.05 (0.37)	-0.33 (0.41)	-0.39 (0.40)	-0.39 (0.40)	-0.39 (0.40)	-0.11 (0.40)
Pearsons cor.	0.73 (0.22)	0.69 (0.25)	-0.14 (0.51)	-0.64 (0.30)	-0.72 (0.21)	-0.72 (0.21)	-0.70 (0.24)	-0.21 (0.28)
Partial cor.	0.00 (0.19)	-0.01 (0.21)	0.01 (0.17)	0.04 (0.18)	0.00 (0.19)	0.00 (0.19)	-0.01 (0.17)	0.00 (0.19)
Circular cor.	0.74 (0.20)	0.71 (0.22)	-0.16 (0.51)	-0.64 (0.29)	-0.73 (0.19)	-0.73 (0.19)	-0.72 (0.21)	-0.22 (0.26)
Coherence	0.12 (0.27)	0.11 (0.27)	-0.12 (0.27)	-0.03 (0.21)	-0.12 (0.27)	-0.12 (0.27)	-0.12 (0.27)	-0.04 (0.26)
Global average <sup>1</sup>	0.40 (0.40)	0.38 (0.40)	-0.10 (0.40)	-0.32 (0.41)	-0.39 (0.40)	-0.39 (0.40)	-0.39 (0.40)	-0.12 (0.40)

<sup>1</sup> Corresponds to an average across all manipulated factors

Table 12

*Average correlation overall and for each level of the manipulated factors (and corresponding standard deviation between parenthesis) for each graph theory measure from weighed networks.*

	Clos. centr.	Global clust. coef.	Avg. strength	Small world coef.	Betw. centr.	Modul.	Charac. path length	Overall
16 electrodes	0.47 (0.41)	0.45 (0.47)	0.38 (0.51)	0.41 (0.39)	-0.30 (0.28)	-0.44 (0.38)	-0.46 (0.40)	0.07 (0.41)
32 electrodes	0.35 (0.35)	0.37 (0.41)	0.30 (0.44)	0.24 (0.39)	-0.15 (0.22)	-0.25 (0.41)	-0.34 (0.34)	0.07 (0.37)
1000 time points	0.30 (0.34)	0.28 (0.38)	0.19 (0.41)	0.33 (0.29)	-0.22 (0.25)	-0.23 (0.30)	-0.30 (0.34)	0.05 (0.33)
10000 time points	0.52 (0.41)	0.54 (0.47)	0.50 (0.49)	0.31 (0.48)	-0.24 (0.28)	-0.46 (0.47)	-0.50 (0.39)	0.10 (0.43)
Ac. temp. of 0.2	0.42 (0.37)	0.40 (0.43)	0.33 (0.47)	0.33 (0.41)	-0.25 (0.24)	-0.36 (0.42)	-0.40 (0.36)	0.07 (0.39)
Ac. temp. of 0.6	0.40 (0.41)	0.42 (0.46)	0.35 (0.49)	0.32 (0.39)	-0.21 (0.29)	-0.33 (0.40)	-0.39 (0.40)	0.08 (0.41)
Ac. spatial of 0.2	0.44 (0.37)	0.44 (0.42)	0.37 (0.48)	0.42 (0.36)	-0.29 (0.28)	-0.36 (0.42)	-0.43 (0.35)	0.08 (0.38)
Ac. spatial of 0.6	0.38 (0.41)	0.38 (0.47)	0.32 (0.48)	0.23 (0.41)	-0.16 (0.22)	-0.32 (0.40)	-0.37 (0.40)	0.07 (0.40)
SNR of 1	0.37 (0.39)	0.38 (0.47)	0.31 (0.51)	0.23 (0.37)	-0.18 (0.22)	-0.30 (0.40)	-0.37 (0.39)	0.06 (0.39)
SNR of 3	0.45 (0.38)	0.44 (0.41)	0.38 (0.45)	0.42 (0.40)	-0.28 (0.29)	-0.39 (0.41)	-0.43 (0.37)	0.08 (0.39)
Pearsons cor.	0.70 (0.23)	0.75 (0.25)	0.68 (0.34)	0.50 (0.41)	-0.36 (0.24)	-0.65 (0.27)	-0.68 (0.22)	0.13 (0.28)
Partial cor.	0.01 (0.16)	0.00 (0.17)	-0.02 (0.17)	0.02 (0.18)	0.01 (0.12)	-0.04 (0.21)	-0.01 (0.16)	-0.00 (0.17)
Circular cor.	0.71 (0.20)	0.75 (0.24)	0.61 (0.43)	0.54 (0.38)	-0.37 (0.21)	-0.64 (0.30)	-0.69 (0.18)	0.13 (0.28)
Coherence	0.22 (0.34)	0.14 (0.42)	0.09 (0.46)	0.24 (0.33)	- (0.31)	-0.04 (0.31)	-0.22 (0.34)	0.07 (0.37)
Global average <sup>1</sup>	0.41 (0.39)	0.41 (0.44)	0.34 (0.48)	0.32 (0.40)	-0.23 (0.26)	-0.34 (0.41)	-0.40 (0.38)	0.07 (0.39)

*Note.* The case with a dash correspond to particular combination of factors where for all data sets of that design cell the graph theory measures had no variance and thus the correlation was not defined.

<sup>1</sup> Corresponds to an average across all manipulated factors

Table 13

*Average correlation overall and for each level of the manipulated factors (and corresponding standard deviation between parenthesis) for each graph theory measure from bipartite networks.*

	Connect.	Cluster coef.	Avg. strength	Betw. centr.	Nestedness	Overall
16 electrodes	0.46 (0.28)	0.42 (0.26)	0.38 (0.51)	-0.30 (0.28)	-0.43 (0.35)	0.11 (0.34)
32 electrodes	0.43 (0.29)	0.41 (0.27)	0.30 (0.44)	-0.15 (0.22)	-0.26 (0.44)	0.15 (0.33)
1000 time points	0.40 (0.31)	0.39 (0.29)	0.19 (0.41)	-0.22 (0.25)	-0.20 (0.33)	0.11 (0.32)
10000 time points	0.48 (0.26)	0.45 (0.23)	0.50 (0.49)	-0.24 (0.28)	-0.49 (0.42)	0.14 (0.34)
Ac. temp. of 0.2	0.44 (0.27)	0.40 (0.27)	0.33 (0.47)	-0.25 (0.24)	-0.35 (0.39)	0.11 (0.33)
Ac. temp. of 0.6	0.44 (0.30)	0.43 (0.26)	0.35 (0.49)	-0.21 (0.29)	-0.34 (0.42)	0.13 (0.35)
Ac. spatial of 0.2	0.43 (0.30)	0.40 (0.27)	0.37 (0.48)	-0.29 (0.28)	-0.37 (0.39)	0.11 (0.34)
Ac. spatial of 0.6	0.45 (0.27)	0.43 (0.26)	0.32 (0.48)	-0.16 (0.22)	-0.32 (0.41)	0.14 (0.33)
SNR of 1	0.47 (0.30)	0.45 (0.27)	0.31 (0.51)	-0.18 (0.22)	-0.32 (0.45)	0.15 (0.35)
SNR of 3	0.41 (0.26)	0.38 (0.25)	0.38 (0.45)	-0.28 (0.29)	-0.38 (0.35)	0.10 (0.32)
Pearsons cor.	0.63 (0.10)	0.59 (0.09)	0.68 (0.34)	-0.36 (0.24)	-0.54 (0.34)	0.20 (0.22)
Partial cor.	0.09 (0.18)	0.09 (0.18)	-0.02 (0.17)	0.01 (0.12)	0.04 (0.21)	0.04 (0.17)
Circular cor.	0.61 (0.11)	0.57 (0.11)	0.61 (0.43)	-0.37 (0.21)	-0.54 (0.32)	0.18 (0.24)
Coherence	-	-	0.09 (0.46)	-	-	0.09 (0.46)
Global average <sup>1</sup>	0.44 (0.28)	0.42 (0.26)	0.34 (0.48)	-0.23 (0.26)	-0.35 (0.40)	0.12 (0.34)

*Note.* The cases with a dash correspond to particular combination of factors where for all data sets of that design cell the graph theory measures had no variance and thus the correlation was not defined.

<sup>1</sup> Corresponds to an average across all manipulated factors

Table 14

*Average correlation overall and for each level of the manipulated factors (and corresponding standard deviation between parenthesis) for each graph theory measure from multiplex networks.*

	Pearsons cor.	Entropy	Global lay coef.	over- clust.	Degree trality	cen- Overall
16 electrodes	0.05 (0.21)	-0.02 (0.17)	-0.01 (0.30)	-0.09 (0.52)	-0.02 (0.30)	
32 electrodes	0.00 (0.20)	0.02 (0.19)	-0.02 (0.34)	0.00 (0.54)	0.00 (0.32)	
1000 time points	0.02 (0.20)	-0.00 (0.19)	-0.04 (0.31)	-0.07 (0.51)	-0.02 (0.30)	
10000 time points	0.04 (0.21)	0.01 (0.18)	0.00 (0.33)	-0.02 (0.55)	0.01 (0.32)	
Ac. temp. of 0.2	0.02 (0.20)	0.02 (0.18)	-0.04 (0.31)	-0.03 (0.52)	-0.01 (0.30)	
Ac. temp. of 0.6	0.03 (0.20)	-0.02 (0.19)	0.00 (0.33)	-0.06 (0.55)	-0.01 (0.32)	
Ac. spatial of 0.2	0.02 (0.21)	0.01 (0.19)	-0.03 (0.27)	-0.05 (0.57)	-0.01 (0.31)	
Ac. spatial of 0.6	0.03 (0.19)	-0.01 (0.18)	-0.01 (0.36)	-0.05 (0.49)	-0.01 (0.30)	
SNR of 1	0.04 (0.22)	-0.01 (0.17)	-0.01 (0.32)	-0.08 (0.53)	-0.01 (0.31)	
SNR of 3	0.01 (0.19)	0.02 (0.19)	-0.03 (0.32)	-0.01 (0.53)	-0.00 (0.31)	
Pearsons cor.	0.01 (0.21)	0.02 (0.22)	0.02 (0.38)	0.03 (0.55)	0.02 (0.34)	
Partial cor.	0.05 (0.22)	0.02 (0.17)	0.02 (0.14)	-0.03 (0.58)	0.02 (0.28)	
Circular cor.	0.02 (0.20)	0.00 (0.16)	-0.10 (0.39)	-0.14 (0.47)	-0.06 (0.30)	
Coherence	0.03 (0.19)	-0.03 (0.19)	-0.01 (0.30)	-0.04 (0.52)	-0.01 (0.30)	
Global average <sup>1</sup>	0.03 (0.20)	0.00 (0.18)	-0.02 (0.32)	-0.05 (0.53)	-0.01 (0.31)	

<sup>1</sup> Corresponds to an average across all manipulated factors

Table 15

*Average correlation overall and for each level of the manipulated factors (and corresponding standard deviation between parenthesis) for each graph theory measure from temporal networks.*

	Density	Clos. centr.	Avg. gree	de- centr.	Betw. centr.	Avg. edge formation	Avg. compo- nent	Overall
16 electrodes	0.21 (0.38)	0.10 (0.05)	0.03 (0.11)	0.07 (0.06)	0.01 (0.03)	-0.07 (0.07)	0.06 (0.12)	
32 electrodes	0.20 (0.28)	0.03 (0.06)	0.03 (0.05)	-0.00 (0.05)	0.01 (0.03)	-0.02 (0.05)	0.04 (0.09)	
1000 time points	0.10 (0.28)	0.06 (0.07)	0.03 (0.11)	0.04 (0.07)	0.01 (0.03)	-0.05 (0.07)	0.03 (0.11)	
10000 time points	0.31 (0.35)	0.06 (0.06)	0.04 (0.05)	0.03 (0.06)	0.02 (0.02)	-0.05 (0.06)	0.07 (0.10)	
Ac. temp. of 0.2	0.23 (0.33)	0.05 (0.06)	0.04 (0.08)	0.03 (0.06)	0.01 (0.03)	-0.05 (0.06)	0.05 (0.10)	
Ac. temp. of 0.6	0.18 (0.34)	0.06 (0.07)	0.03 (0.08)	0.04 (0.07)	0.01 (0.03)	-0.05 (0.07)	0.04 (0.11)	
Ac. spatial of 0.2	0.19 (0.35)	0.06 (0.07)	0.03 (0.08)	0.03 (0.07)	0.01 (0.03)	-0.05 (0.07)	0.04 (0.11)	
Ac. spatial of 0.6	0.22 (0.32)	0.06 (0.06)	0.03 (0.09)	0.04 (0.06)	0.01 (0.03)	-0.05 (0.06)	0.05 (0.10)	
SNR of 1	0.13 (0.37)	0.04 (0.06)	0.01 (0.10)	0.02 (0.06)	0.01 (0.03)	-0.03 (0.06)	0.03 (0.11)	
SNR of 3	0.28 (0.28)	0.08 (0.06)	0.05 (0.05)	0.05 (0.07)	0.02 (0.03)	-0.07 (0.07)	0.07 (0.09)	
Pearsons cor.	0.34 (0.35)	0.08 (0.06)	0.06 (0.07)	0.06 (0.07)	0.02 (0.02)	-0.07 (0.06)	0.08 (0.10)	
Partial cor.	-0.03 (0.18)	-0.01 (0.04)	-0.00 (0.04)	0.01 (0.03)	-0.00 (0.03)	-0.00 (0.04)	-0.01 (0.06)	
Circular cor.	0.36 (0.33)	0.09 (0.07)	0.06 (0.10)	0.06 (0.08)	0.02 (0.02)	-0.08 (0.07)	0.08 (0.11)	
Coherence	0.15 (0.30)	0.04 (0.04)	0.02 (0.10)	0.00 (0.05)	0.02 (0.03)	-0.04 (0.03)	0.03 (0.09)	
Global average <sup>1</sup>	0.21 (0.33)	0.06 (0.07)	0.03 (0.08)	0.03 (0.07)	0.01 (0.03)	-0.05 (0.06)	0.05 (0.11)	

<sup>1</sup> Corresponds to an average across all manipulated factors

## C Mixed model ANOVA

Table 16

*Mixed model ANOVA results (using all manipulated factors)*

	Sum Sq	num Df	Error SS	den Df	F value	Pr(>F) <sup>1</sup>	
(Intercept)	615.50	1.00	0.01	1.00	68848.34	0.0024	**
n_electrodes	11.07	1.00	0.01	1.00	1238.15	0.018	*
n_time_points	50.75	1.00	0.01	1.00	5677.10	0.0084	**
signal_to_noise	0.25	1.00	0.01	1.00	28.23	0.12	
autocor_temporel	0.32	1.00	0.01	1.00	35.39	0.11	
autocor_spatial	0.31	1.00	0.01	1.00	34.82	0.11	
n_electrodes × n_time_points	0.93	1.00	0.01	1.00	103.97	0.062	.
n_electrodes × signal_to_noise	0.07	1.00	0.01	1.00	7.75	0.22	
n_time_points × signal_to_noise	0.00	1.00	0.01	1.00	0.29	0.69	
n_electrodes × autocor_temporel	0.00	1.00	0.01	1.00	0.01	0.95	
n_time_points × autocor_temporel	0.00	1.00	0.01	1.00	0.03	0.89	
signal_to_noise × autocor_temporel	0.00	1.00	0.01	1.00	0.33	0.67	
n_electrodes × autocor_spatial	0.62	1.00	0.01	1.00	69.30	0.076	.
n_time_points × autocor_spatial	0.00	1.00	0.01	1.00	0.07	0.84	
signal_to_noise × autocor_spatial	0.01	1.00	0.01	1.00	0.97	0.5	
autocor_temporel × autocor_spatial	0.02	1.00	0.01	1.00	1.69	0.42	
n_electrodes × n_time_points × signal_to_noise	0.00	1.00	0.01	1.00	0.11	0.8	
n_electrodes × n_time_points × autocor_temporel	0.04	1.00	0.01	1.00	3.98	0.3	
n_electrodes × signal_to_noise × autocor_temporel	0.10	1.00	0.01	1.00	11.21	0.18	
n_time_points × signal_to_noise × autocor_temporel	0.69	1.00	0.01	1.00	77.60	0.072	.
n_electrodes × n_time_points × autocor_spatial	0.09	1.00	0.01	1.00	10.38	0.19	
n_electrodes × signal_to_noise × autocor_spatial	0.08	1.00	0.01	1.00	8.85	0.21	
n_time_points × signal_to_noise × autocor_spatial	0.01	1.00	0.01	1.00	0.75	0.55	
n_electrodes × autocor_temporel × autocor_spatial	0.01	1.00	0.01	1.00	1.55	0.43	
n_time_points × autocor_temporel × autocor_spatial	0.04	1.00	0.01	1.00	4.21	0.29	
signal_to_noise × autocor_temporel × autocor_spatial	0.49	1.00	0.01	1.00	55.09	0.085	.
n_electrodes × n_time_points × signal_to_noise × autocor_temporel	0.09	1.00	0.01	1.00	9.88	0.2	
n_electrodes × n_time_points × signal_to_noise × autocor_spatial	0.03	1.00	0.01	1.00	2.94	0.34	
n_electrodes × n_time_points × autocor_temporel × autocor_spatial	0.43	1.00	0.01	1.00	48.00	0.091	.
n_electrodes × signal_to_noise × autocor_temporel × autocor_spatial	0.01	1.00	0.01	1.00	1.18	0.47	

<sup>1</sup> The presented p-values are adjusted with the Greenhouse-Geisser correction  $\hat{\epsilon}$  for lack of sphericity, which is the case for all effects with more than one degree of freedom in the numerator.

.  $p < 0.1$ . \* $p < 0.05$ . \*\* $p < 0.01$ . \*\*\*  $p < 0.001$ .

	Sum Sq	num Df	Error SS	den Df	F value	Pr(>F) <sup>1</sup>
n_time_points × signal_to_noise × autocor_tempore l × autocor_spatial	0.01	1.00	0.01	1.00	1.23	0.47
measure	218.99	21.00	1.63	21.00	134.34	0.055
n_electrodes × measure	6.65	21.00	1.63	21.00	4.08	0.29
n_time_points × measure	43.33	21.00	1.63	21.00	26.58	0.12
signal_to_noise × measure	1.50	21.00	1.63	21.00	0.92	0.51
autocor_temporel × measure	0.39	21.00	1.63	21.00	0.24	0.71
autocor_spatial × measure	0.69	21.00	1.63	21.00	0.42	0.63
n_electrodes × n_time_points × measure	2.70	21.00	1.63	21.00	1.66	0.42
n_electrodes × signal_to_noise × measure	0.97	21.00	1.63	21.00	0.60	0.58
n_time_points × signal_to_noise × measure	1.43	21.00	1.63	21.00	0.87	0.52
n_electrodes × autocor_temporel × measure	0.32	21.00	1.63	21.00	0.20	0.73
n_time_points × autocor_temporel × measure	0.78	21.00	1.63	21.00	0.48	0.61
signal_to_noise × autocor_temporel × measure	0.30	21.00	1.63	21.00	0.18	0.74
n_electrodes × autocor_spatial × measure	0.58	21.00	1.63	21.00	0.36	0.66
n_time_points × autocor_spatial × measure	0.32	21.00	1.63	21.00	0.20	0.73
signal_to_noise × autocor_spatial × measure	0.85	21.00	1.63	21.00	0.52	0.6
autocor_temporel × autocor_spatial × measure	0.67	21.00	1.63	21.00	0.41	0.64
n_electrodes × n_time_points × signal_to_noise × measure	2.00	21.00	1.63	21.00	1.22	0.47
n_electrodes × n_time_points × autocor_temporel × measure	0.93	21.00	1.63	21.00	0.57	0.59
n_electrodes × signal_to_noise × autocor_temporel × measure	0.28	21.00	1.63	21.00	0.17	0.75
n_time_points × signal_to_noise × autocor_temporel × measure	0.72	21.00	1.63	21.00	0.44	0.63
n_electrodes × n_time_points × autocor_spatial × measure	0.66	21.00	1.63	21.00	0.40	0.64
n_electrodes × signal_to_noise × autocor_spatial × measure	0.89	21.00	1.63	21.00	0.55	0.59
n_time_points × signal_to_noise × autocor_spatial × measure	0.46	21.00	1.63	21.00	0.28	0.69
n_electrodes × autocor_temporel × autocor_spatial × measure	0.74	21.00	1.63	21.00	0.45	0.62
n_time_points × autocor_temporel × autocor_spatial × measure	0.28	21.00	1.63	21.00	0.17	0.75
signal_to_noise × autocor_temporel × autocor_spatial × measure	1.13	21.00	1.63	21.00	0.69	0.56
n_electrodes × n_time_points × signal_to_noise × autocor_temporel × measure	0.54	21.00	1.63	21.00	0.33	0.67
n_electrodes × n_time_points × signal_to_noise × autocor_spatial × measure	1.01	21.00	1.63	21.00	0.62	0.57
n_electrodes × n_time_points × autocor_temporel × autocor_spatial × measure	1.07	21.00	1.63	21.00	0.65	0.57
n_electrodes × signal_to_noise × autocor_temporel × autocor_spatial × measure	0.39	21.00	1.63	21.00	0.24	0.71
n_time_points × signal_to_noise × autocor_temporel × autocor_spatial × measure	0.64	21.00	1.63	21.00	0.39	0.64
transform_function	99.69	3.00	0.20	3.00	497.76	0.029 *
n_electrodes × transform_function	4.34	3.00	0.20	3.00	21.69	0.13
n_time_points × transform_function	16.02	3.00	0.20	3.00	80.00	0.071
signal_to_noise × transform_function	0.68	3.00	0.20	3.00	3.39	0.32
autocor_temporel × transform_function	0.11	3.00	0.20	3.00	0.57	0.59

<sup>1</sup> The presented p-values are adjusted with the Greenhouse-Geisser correction  $\hat{\epsilon}$  for lack of sphericity, which is the case for all effects with more than one degree of freedom in the numerator.

.  $p < 0.1$ . \* $p < 0.05$ . \*\* $p < 0.01$ . \*\*\*  $p < 0.001$ .

	Sum Sq	num Df	Error SS	den Df	F value	Pr(>F) <sup>1</sup>
autocor_spatial × transform_function	0.34	3.00	0.20	3.00	1.69	0.42
n_electrodes × n_time_points × transform_function	0.86	3.00	0.20	3.00	4.29	0.29
n_electrodes × signal_to_noise × transform_function	0.10	3.00	0.20	3.00	0.50	0.61
n_time_points × signal_to_noise × transform_function	0.16	3.00	0.20	3.00	0.80	0.54
n_electrodes × autocor_temporel × transform_function	0.27	3.00	0.20	3.00	1.34	0.45
n_time_points × autocor_temporel × transform_function	0.05	3.00	0.20	3.00	0.23	0.72
signal_to_noise × autocor_temporel × transform_function	0.09	3.00	0.20	3.00	0.46	0.62
n_electrodes × autocor_spatial × transform_function	0.39	3.00	0.20	3.00	1.97	0.39
n_time_points × autocor_spatial × transform_function	0.03	3.00	0.20	3.00	0.17	0.75
signal_to_noise × autocor_spatial × transform_function	0.01	3.00	0.20	3.00	0.05	0.86
autocor_temporel × autocor_spatial × transform_function	0.20	3.00	0.20	3.00	1.00	0.5
n_electrodes × n_time_points × signal_to_noise × transform_function	0.40	3.00	0.20	3.00	1.99	0.39
n_electrodes × n_time_points × autocor_temporel × transform_function	0.14	3.00	0.20	3.00	0.68	0.56
n_electrodes × signal_to_noise × autocor_temporel × transform_function	0.16	3.00	0.20	3.00	0.79	0.54
n_time_points × signal_to_noise × autocor_temporel × transform_function	0.52	3.00	0.20	3.00	2.57	0.35
n_electrodes × n_time_points × autocor_spatial × transform_function	0.00	3.00	0.20	3.00	0.01	0.93
n_electrodes × signal_to_noise × autocor_spatial × transform_function	0.15	3.00	0.20	3.00	0.75	0.55
n_time_points × signal_to_noise × autocor_spatial × transform_function	0.28	3.00	0.20	3.00	1.38	0.45
n_electrodes × autocor_temporel × autocor_spatial × transform_function	0.23	3.00	0.20	3.00	1.16	0.48
n_time_points × autocor_temporel × autocor_spatial × transform_function	0.22	3.00	0.20	3.00	1.10	0.49
signal_to_noise × autocor_temporel × autocor_spatial × transform_function	0.05	3.00	0.20	3.00	0.24	0.71
n_electrodes × n_time_points × signal_to_noise × autocor_temporel × transform_function	0.15	3.00	0.20	3.00	0.76	0.54
n_electrodes × n_time_points × signal_to_noise × autocor_spatial × transform_function	0.03	3.00	0.20	3.00	0.14	0.77
n_electrodes × n_time_points × autocor_temporel × autocor_spatial × transform_function	0.22	3.00	0.20	3.00	1.12	0.48
n_electrodes × signal_to_noise × autocor_temporel × autocor_spatial × transform_function	0.14	3.00	0.20	3.00	0.71	0.55
n_time_points × signal_to_noise × autocor_temporel × autocor_spatial × transform_function	0.04	3.00	0.20	3.00	0.18	0.74
measure × transform_function	115.73	63.00	2.94	63.00	39.33	0.1
n_electrodes × measure × transform_function	11.41	63.00	2.94	63.00	3.88	0.3
n_time_points × measure × transform_function	35.57	63.00	2.94	63.00	12.09	0.18
signal_to_noise × measure × transform_function	7.51	63.00	2.94	63.00	2.55	0.36
autocor_temporel × measure × transform_function	1.48	63.00	2.94	63.00	0.50	0.61
autocor_spatial × measure × transform_function	2.48	63.00	2.94	63.00	0.84	0.53
n_electrodes × n_time_points × measure × transform_function	8.45	63.00	2.94	63.00	2.87	0.34
n_electrodes × signal_to_noise × measure × transform_function	2.28	63.00	2.94	63.00	0.78	0.54
n_time_points × signal_to_noise × measure × transform_function	4.51	63.00	2.94	63.00	1.53	0.43
n_electrodes × autocor_temporel × measure × transform_function	2.14	63.00	2.94	63.00	0.73	0.55
n_time_points × autocor_temporel × measure × transform_function	1.72	63.00	2.94	63.00	0.58	0.58

<sup>1</sup> The presented p-values are adjusted with the Greenhouse-Geisser correction  $\hat{\epsilon}$  for lack of sphericity, which is the case for all effects with more than one degree of freedom in the numerator.

.  $p < 0.1$ . \* $p < 0.05$ . \*\* $p < 0.01$ . \*\*\*  $p < 0.001$ .

	Sum Sq	num Df	Error SS	den Df	F value	Pr(>F) <sup>1</sup>
signal_to_noise × autocor_temporel × measure × transform_function	1.26	63.00	2.94	63.00	0.43	0.63
n_electrodes × autocor_spatial × measure × transform_function	2.31	63.00	2.94	63.00	0.78	0.54
n_time_points × autocor_spatial × measure × transform_function	1.33	63.00	2.94	63.00	0.45	0.62
signal_to_noise × autocor_spatial × measure × transform_function	1.66	63.00	2.94	63.00	0.56	0.59
autocor_temporel × autocor_spatial × measure × transform_function	4.56	63.00	2.94	63.00	1.55	0.43
n_electrodes × n_time_points × signal_to_noise × measure × transform_function	3.48	63.00	2.94	63.00	1.18	0.47
n_electrodes × n_time_points × autocor_temporel × measure × transform_function	1.79	63.00	2.94	63.00	0.61	0.58
n_electrodes × signal_to_noise × autocor_temporel × measure × transform_function	1.81	63.00	2.94	63.00	0.61	0.58
n_time_points × signal_to_noise × autocor_temporel × measure × transform_function	3.24	63.00	2.94	63.00	1.10	0.48
n_electrodes × n_time_points × autocor_spatial × measure × transform_function	2.27	63.00	2.94	63.00	0.77	0.54
n_electrodes × signal_to_noise × autocor_spatial × measure × transform_function	1.89	63.00	2.94	63.00	0.64	0.57
n_time_points × signal_to_noise × autocor_spatial × measure × transform_function	2.98	63.00	2.94	63.00	1.01	0.5
n_electrodes × autocor_temporel × autocor_spatial × measure × transform_function	3.28	63.00	2.94	63.00	1.11	0.48
n_time_points:autocor_temporel × autocor_spatial × measure × transform_function	1.86	63.00	2.94	63.00	0.63	0.57
signal_to_noise × autocor_temporel × autocor_spatial × measure × transform_function	1.92	63.00	2.94	63.00	0.65	0.57
n_electrodes × n_time_points × signal_to_noise × autocor_temporel × measure × transform_function	1.48	63.00	2.94	63.00	0.50	0.61
n_electrodes × n_time_points × signal_to_noise × autocor_spatial × measure × transform_function	2.67	63.00	2.94	63.00	0.91	0.52
n_electrodes × n_time_points × autocor_temporel × autocor_spatial × measure × transform_function	5.09	63.00	2.94	63.00	1.73	0.41
n_electrodes × signal_to_noise × autocor_temporel × autocor_spatial × measure × transform_function	1.78	63.00	2.94	63.00	0.60	0.58
n_time_points × signal_to_noise × autocor_temporel × autocor_spatial × measure × transform_function	1.72	63.00	2.94	63.00	0.58	0.58

<sup>1</sup> The presented p-values are adjusted with the Greenhouse-Geisser correction  $\hat{\epsilon}$  for lack of sphericity, which is the case for all effects with more than one degree of freedom in the numerator.

.  $p < 0.1$ . \* $p < 0.05$ . \*\* $p < 0.01$ . \*\*\*  $p < 0.001$ .

## D Mixed model ANOVA 2

Table 17

Mixed model ANOVA results (excluding the temporal and spatial autocorrelation factor).

	Sum Sq	num Df	Error SS	den Df	F value	Pr(>F) <sup>1</sup>	$\eta_G^2$
(Intercept)	615.50	1.00	3.40	24.00	4343.24	1.2e-28 ***	0.98
<b>n_electrodes</b>	11.07	1.00	3.40	24.00	78.11	5.2e-09 ***	0.50
<b>n_timepoints</b>	50.75	1.00	3.40	24.00	358.14	6.3e-16 ***	0.82
signal_to_noise	0.25	1.00	3.40	24.00	1.78	0.19	0.02
n_electrodes × n_timepoints	0.93	1.00	3.40	24.00	6.56	0.017 *	0.08
n_electrodes × signal_to_noise	0.07	1.00	3.40	24.00	0.49	0.49	0.01
n_timepoints × signal_to_noise	0.00	1.00	3.40	24.00	0.02	0.89	0.00
n_electrodes × n_timepoints × signal_to_noise	0.00	1.00	3.40	24.00	0.01	0.94	0.00
<b>measure</b>	218.99	21.00	16.27	504.00	323.08	8.8e-80 ***	0.80
n_electrodes × measure	6.65	21.00	16.27	504.00	9.81	5.9e-09 ***	0.11
<b>n_timepoints × measure</b>	43.33	21.00	16.27	504.00	63.92	1.2e-37 ***	0.45
signal_to_noise × measure	1.50	21.00	16.27	504.00	2.21	0.046 *	0.03
n_electrodes × n_timepoints × measure	2.70	21.00	16.27	504.00	3.99	0.0011 **	0.05
n_electrodes × signal_to_noise × measure	0.97	21.00	16.27	504.00	1.44	0.21	0.02
n_timepoints × signal_to_noise × measure	1.43	21.00	16.27	504.00	2.10	0.057 .	0.03
n_electrodes × n_timepoints × signal_to_noise × measure	2.00	21.00	16.27	504.00	2.95	0.01 *	0.04
<b>transform_function</b>	99.69	3.00	4.02	72.00	595.14	1.3e-43 ***	0.88
n_electrodes × transform_function	4.34	3.00	4.02	72.00	25.93	4.1e-10 ***	0.25
<b>n_timepoints × transform_function</b>	16.02	3.00	4.02	72.00	95.65	1e-21 ***	0.55
signal_to_noise × transform_function	0.68	3.00	4.02	72.00	4.05	0.015 *	0.05
n_electrodes × n_timepoints × transform_function	0.86	3.00	4.02	72.00	5.13	0.0049 **	0.06
n_electrodes × signal_to_noise × transform_function	0.10	3.00	4.02	72.00	0.60	0.59	0.01
n_timepoints × signal_to_noise × transform_function	0.16	3.00	4.02	72.00	0.96	0.41	0.01
n_electrodes × n_timepoints × signal_to_noise × transform_function	0.40	3.00	4.02	72.00	2.38	0.088 .	0.03
<b>measure × transform_function</b>	115.73	63.00	55.64	1512.00	49.92	1.6e-41 ***	0.39
n_electrodes × measure × transform_function	11.41	63.00	55.64	1512.00	4.92	2e-05 ***	0.06
n_timepoints × measure × transform_function	35.57	63.00	55.64	1512.00	15.34	8.2e-17 ***	0.16
signal_to_noise × measure × transform_function	7.51	63.00	55.64	1512.00	3.24	0.002 **	0.04
n_electrodes × n_timepoints × measure × transform_function	8.45	63.00	55.64	1512.00	3.64	0.00068 ***	0.04

<sup>1</sup> The presented p-values are adjusted with the Greenhouse-Geisser correction  $\hat{\epsilon}$  for lack of sphericity, which is the case for all effects with more than one degree of freedom in the numerator.

Effects with a generalized eta squared above .26 are in bold.

.  $p < 0.1$ . \* $p < 0.05$ . \*\* $p < 0.01$ . \*\*\*  $p < 0.001$ .

	Sum Sq	num Df	Error SS	den Df	F value	Pr(>F) <sup>1</sup>	$\eta_G^2$
n_electrodes × signal_to_noise × measure × transform_function	2.28	63.00	55.64	1512.00	0.99	0.45	0.01
n_timepoints × signal_to_noise × measure × transform_function	4.51	63.00	55.64	1512.00	1.95	0.058 .	0.02
n_electrodes × n_timepoints × signal_to_noise × measure × transform_function	3.48	63.00	55.64	1512.00	1.50	0.16	0.02

<sup>1</sup> The presented p-values are adjusted with the Greenhouse-Geisser correction  $\hat{\epsilon}$  for lack of sphericity, which is the case for all effects with more than one degree of freedom in the numerator.

Effects with a generalized eta squared above .26 are in bold.

.  $p < 0.1$ . \* $p < 0.05$ . \*\* $p < 0.01$ . \*\*\*  $p < 0.001$ .